Making Materials Which Feel Warm to the Touch by Incorporation of Aerogels

by

Abdullah Göktuğ Gönel

A Thesis Submitted to the
Graduate School of Sciences and Engineering
in Partial Fulfillment of the Requirements for
the Degree of

Master of Science
in
Chemical and Biological Engineering

Koç University

August 2016

Koç University

Graduate School of Sciences and Engineering

This is to certify that I have examined this copy of a master's thesis by

Abdullah Göktuğ Gönel

and have found that it is complete and satisfactory in all respects,
and that any and all revisions required by the final
examining committee have been made.

Committee Members:

_____

Can Erkey, Ph. D. (Advisor)

_____

Seda Kızılel, Ph. D.

_____

Ayşe Bayrakçeken Yurtcan, Ph. D.

Date: 31/08/2016

to my family…

ABSTRACT

The warm sensation is related to the amount of heat extracted from the human skin when it is in contact with a material. This heat extraction can be described by the time dependent heat flux which occurs from the skin to the object. The heat flux depends on the material properties such as thermal conductivity, density and heat capacity. Increasing warm sensation requires decreasing these properties. Urea formaldehyde is a thermoplastic polymer which is most commonly used to make toilet seats. Improving warm sensation of toilet seat has become a good marketing strategy. To enhance the thermal comfort of the seats electric heaters are currently in use. However it raises safety issues because of high possibility of water contact with the heater. This project aims to give the urea formaldehyde based toilet seats to warm sensation by incorporating aerogels which exhibits high resistance to heat flow. Urea formaldehyde grains were mixed with aerogels (silica and resorcinol formaldehyde aerogels) and hot pressed together to obtain an aerogel incorporated composite. Composites were manufactured by hot pressing this mixture at elevated pressures and temperatures in the industrial size hot press molds at the manufacture site of toilet seats. Thermal conductivity and density of the composites were measured. Changes in aerogels' density and pore properties were determined at different pressures with a laboratory scale cold press. Denser aerogels were synthesized to make aerogels more resistant to the composite manufacture pressure. Composites with dense aerogels (0.361-0.48 g/cm^3) successfully reduced the thermal conductivity of native urea formaldehyde by up to 40% by using volume fractions up to 0.38. With reduced contact coefficient parameters, up to 45% reduction in the heat flux was obtained. Thermal conductivity of composites was also predicted with effective thermal conductivity models such as Maxwell and effective medium theory (EMT). At lower volume fractions Maxwell and Rayleigh models gave good predictions for the composite thermal conductivity. Effective thermal conductivity of composites with dense silica aerogels were best predicted with EMT.

ÖZET

Bir malzemenin ılık hissiyatı, insan dersinden temas halinde olan objeye geçen ısı miktarı ile doğrudan ilintilidir. Deriden objeye aktarılan ısı miktarı ve bu ısının zamana göre değişimi kararsız ısı iletim denklemlerinin kullanılmasıyla elde edilen ısı akısı ile tanımlanabilir. Bu ısı akısı malzemenin yoğunluğu, ısı iletim katsayısı ve ısı sığası gibi özellikleri ile değişiklik gösterir. Bir objeye kazandırılacak ılık hissiyatı, malzemenin bu özelliklerinin düşürülmesi ile mümkün. Üre formaldehit klozet oturakları yapımında sıklıkla kullanılan bir termoplastiktir. Klozet oturaklarını ılık hale getirmek iyi bir pazarlama stratejisi haline gelmiştir. Bu oturakların ısıl konforunu arttırmak için piyasada hali hazırda elektrikli ısıtıcılar kullanılmaktadır. Ancak su temas riskinin yüksek olduğu yaşam alanlarında, bu elektrikli ısıtıcıları kullanmak tehlike arz etmektedir. Bu tez üreformaldehit polimerinin ısı akışına direnç gösteren aerojel malzemeleri ile kompozitini üreterek, dışarıdan ısı sağlanmaksızın, ılık hisli klozet kapakları üretmeyi hedeflemektedir. Bu hedefi gerçekleştirmek üzere üre formaldehit granülleri, aerojel parçacıkları (silika ve rezorsinol formaldehit aerojeller) ile karıştırılarak sıcak preste kompozitler üretilmiştir. Kompozitlerin üretimi, oturak üretimin gerçekleştiği fabrikadaki endüstriyel sıcak preslerde gerçekleştirilmiştir. Elde edilen kompozitlerin ısı iletim katsayısı ve özgül ağırlıkları ölçüldü. Basınca maruz kalan aerojellerin gözenek yapısındaki ve özgül ağırlarındaki değişimi gözlemlemek için laboratuvar ölçeklerinde pres kullanıldı. Özgül ağırlığı daha fazla olan, üretim basıncına daha dayanıklı olabileceği öngörülen aerojeller kompozitlerde kullanılmak üzere sentezlendi. Yoğunluğu fazla aerojllerin (0.361-0.48 g/cm^3) 0.38 hacimsel oranlarına kadar kullanılan kompozitleri ısı iletim katsayısında %40'lık düşüş sağladı. Isı akısını etkileyen, malzemenin özelliklerindeki düşüşle ısı akısında %45'liğe kadar bir düşüş elde edildi. Oluşturulan kompozitlerin etkin ısı katsayıları modellerle tahmin edildi. Maxwell, Rayleigh ve etkin ortam kuramı modelleri kullanıldı. Kullanılan modeller arasında Maxwell ve Rayleigh düşük hacimsel aerojel fraksiyonlarına sahip kompozitlerde , etkin ortam kuramı ise yüksek fraksiyonlara sahip kompozitlerde iyi tahminler verdi.

ACKNOWLEDGEMENTS

I would like to express my deepest gratitude to my advisor, Prof Can Erkey who has been a great academic mentor for both my undergraduate and graduate study. I am truly thankful for his encouragement, enthusiasm and patience. I am really grateful for the erudite and casual discussion sessions with him. I will undoubtedly miss our travels to the factory and conferences. These journeys has always been fun and illuminating.

I also would like to sincerely thank to my thesis committee members, Assoc. Prof. Seda Kızılel and Assoc. Prof. Ayşe Bayrakçeken for sparing their valuable time for me. I am also truly greatful for Dr Kızılel's informative lectures which I took during my undergraduate and graduate years.

I would like thank my current and previous colleagues Dr. Selmi Erim Bozbağ, Dr Deniz Şanlı Yıldız, Dr. Zeynep Ülker Demir, Yaprak Özbakır, Ezgi Erdem, Metin Karayılan, Ramazan Oğuz Canıaz, İbrahim Şahin, Gamze Eriş, Seçil Ünsal, Hazal Karadağ, Muhammed Anas, Shadi Khan Baloch, Bengisu Barım, Umaima Saleem, Zeynep İnönü, Salim Şimşek and Ayşegül Bayat for sustaining quite lively and inductive research environment.

My sincere thanks also go for my dear friends Selen Manioğlu, Volkan Balci, Ehsan Sarayloo, Elda Beruhil Adatoz, Fatih Rahim, Gokhan Gecer, Mehmet Emre Çetinkaya, Pelin Erkoç and Dilem Oran for the enjoyable times we had.

I would like to especially thank my family for their endless love, support and encouragement.

This thesis is an Industrial Thesis Project (San-Tez) (0489.STZ.2013-2), funded by Republic of Turkey Ministry of Science, Industry and Technology and our industry partner Eczacıbaşı Vitra Ltd.

TABLE OF CONTENTS

LIST OF TABLES

LIST OF FIGURES

NOMENCLATURE

k	*thermal conductivity*
c_p	*heat capacity*
ρ	*density*
UF	*urea formaldehyde*
RFA	*resorcinol formaldehyde*
$q_s^{"}$	*heat flux at the surface*
SA	*silica aerogel*
RFA-H	*resorcinol formaldehyde with bulk higher density*
SA-H	*silica aerogel with higher bulk*

Chapter 1 Introduction

There is a need to develop materials which feel warm to the touch. This need emerges because improving the ergonomics and thermal comfort for materials (such as bathroom tiles and other ceramic based products) have become good marketing point for the manufacturers. Increasing thermal comfort is especially important for those who are sensitive to cold. The target of such products specifically include elderly in nursing homes, patients in hospitals and people with rheumatic disorders. This study was conducted with the partnership of Eczacıbaşı Vitra Ltd. to create warm feeling toilet seats. According to Eczacıbaşı Vitra's customer survey, there is a great discomfort in cold weathers in restrooms for the customer when they contact with the surrounding objects, especially the toilet seats. The current solution to the problem is the usage of electrical heating circuits which are embedded under the seat. However this rises a safety concern because the restroom area is a water abundant environment and water contact with the thermal resistant could be quite dangerous. Therefore warm to the touch toilet seat production is a good solution for the current problem. Urea-formaldehyde (UF) polymer is commonly used for the manufacture toilet seats in the industry. It is also the polymer used by our industry partner in this project. In order to make UF warm to the touch, it is important to know how exactly warmness and coldness is perceived by human body.

When there is a temperature gradient between the human skin and the object heat transfer occurs. If the material has a lower temperature, heat will be extracted from the skin. The amount of heat extracted is directly related with the sensation of warmness and coldness. The heat flux from the skin to the material is time dependent because the human skin maintains a constant temperature (around 34°C) by the constant blood flow [1-5]. Therefore eventually temperature equilibrium between the object and the skin is sustained. Time dependent behavior of heat flux is defined as cooling curve. Cooling curve has a high initial value and exponentially decays to zero heat flux. This implies that the great portion of heat transfer occurs in the very

first part of the cooling curve in a very short amount of time, usually reported within a second [2]. The heat transfer between to the human skin and the material which are in contact can be described by the transient heat of conduction equation. The solution of the equation relates the heat flux with the bulk properties of the material which is being touched (1.1). Heat flux depends on the skin temperature (T_i) and the initial temperature of the object's surface. The part of the solution which is directly related to the material is defined as contact coefficient or thermal absorptivity. Contact coefficient is the square root of the products of thermal conductivity (k), heat capacity (c_p) and the density (ρ) of the material. This dependence implies even if a hand touches different object at the same temperature, perception of warmness or coldness would be different since these materials have a different contact coefficient. This could be also observed in an everyday phenomena. For example when one touches wood and metal at the same temperature, thermal sensation is different.

$$q_s^{"} = \sqrt{k.\rho.c_p} \times \frac{(T_i - T_s)}{\sqrt{\pi.t}} \quad (1.1)$$

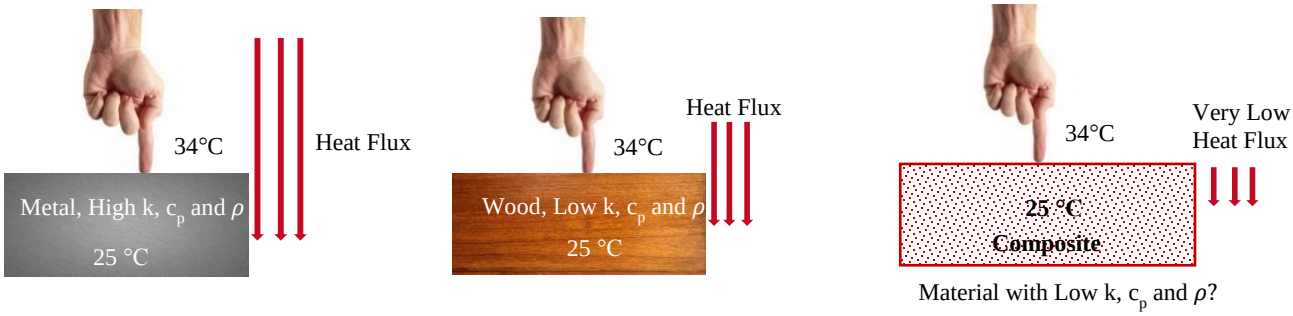

Figure 1-1: Initial heat flux magnitude for different materials which are at the same temperature

Touching a metal piece at room temperature feels colder as compared touching a piece of wood at the same temperature. The reason for this relative perception coldness for the metal is that it has high contact coefficient and consequently higher initial heat flux. The magnitude of initial heat flux is lower for the wood because it has a lower k, c_p and ρ values. This results

suggest if a composite of UF with a very low k, cp and ρ can be manufactured, then a toilet which feel warm to the touch can be obtained.

One way to make UF warm to the touch, is to incorporate particles which have low thermal conductivity. UF based products are obtained by compressing the UF grains in stainless steel molds at elevated pressures and temperatures. After hot pressing the grains, hard textured materials are obtained in the shape of the stainless steel mold. Thermal conductivity of urea formaldehyde is around 450 mW/m.K with a density usually around 1.4 g/mL [6]. An aerogels is a good candidate to reduce the thermal conductivity and density of the UF. Aerogels are nanostructured materials which attracted a lot research attention due to their properties such as low thermal conductivity (10–100 mW/m.K), high porosity (80-99%), low density (0.01–0.5 g/cm3) and high surface area (100-1000 m2/g) [7]. Aerogels are synthesized through sol-gel process and during the synthesis pore properties can be tuned easily by changing the sol-gel parameters which in turns changes the thermal and mechanical properties of aerogels [7-9]. Because of their low thermal conductivity and density, aerogels are extremely warmer to the touch. With the incorporation of aerogels in UF matrix, the initial heat flux can be reduced. Comparison of cooling curves of pure UF and pure aerogel (resorcinol formaldehyde aerogel (RFA)) is given in the Figure 2. The initial surface heat flux ratio (1.2) of UF to RFA is 35.

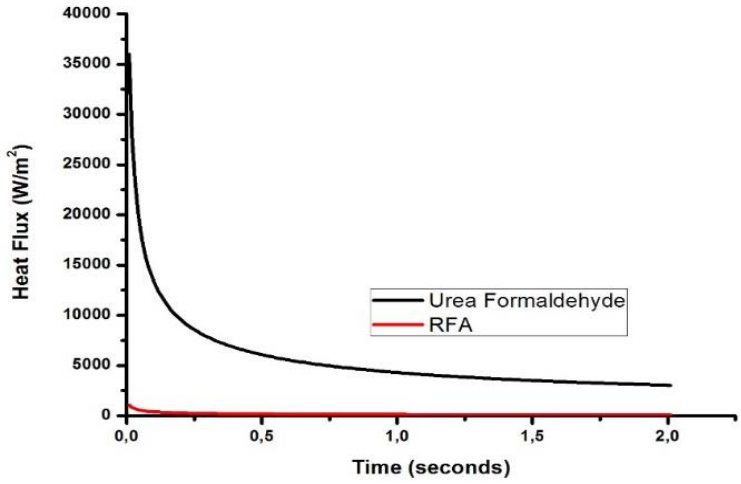

Figure 1-2: *Comparison of change in the heat flux when the object is pure UF and pure aerogel*

$$\frac{q''_{s,UF}}{q''_{RFA}} = \frac{\sqrt{k_{UF} \cdot \rho_{UF} \cdot c_{p,UF}}}{\sqrt{k_{RFA} \cdot \rho_{RFA} \cdot c_{p,RFA}}} \quad (2.2)$$

To the best of knowledge, there is there is no urea-formaldehyde and aerogel composite present in the literature. The objective of this project is to incorporate aerogels into urea formaldehyde polymer to obtain a composite which feels warmer to the touch compare to the native urea formaldehyde polymer plates. Chapter 2 presents a review of warm sensation studies, aerogels synthesis, urea formaldehyde production, composites of aerogels and effective thermal conductivity prediction models. In Chapter 3 experimental methodology is covered. The chemicals used in the project, how aerogels synthesized, composite preparation are presented in this chapter. The methodology used to characterize the aerogel and composite samples are described. Chapter 4 shows the results of pressure effect on the structure of various aerogels, thermal conductivity and density of prepared composites and also the predictions of the effective thermal conductivity. Chapter 5 concludes the thesis by summarizing the work done.

Chapter 2 Literature Review

2.1 Perception of Warmness

Thermal sensation is an important part of the human regulatory system. It helps humans to identify the surrounding and makes body to take actions accordingly. Under the epidermis there are thermoreceptors which send signals to central nervous system the temperature gradient existing between the dermis and the environment or the materials which are in contact with the skin. Temperature perception of human body has evolved to sense very small temperature difference as small as 0.02°C [10].

Perception of warmness is studied in various research field ranging from medical sciences to engineering. The fields that investigate the human heat sensation in the similar fashion of this thesis include haptic science and technology and textiles. In haptic technology, the goal is to develop an understanding of how warmness and coldness is perceived to create devices which enables users to experience virtual reality[11]. Along with other tactile sensations such as roughness, stiffness, perception of heat is used to identify various objects. This is used in the field of robotics to develop more human-like smart and sensitive robots[12]. In textiles, there are limited number of studies on which fabrics give warm sensation in cold environments [13, 14]. Models are developed to correlate the temperature of the environment and the physical properties of fluids or solid objects that are in contact with skin to evaluate what is actually perceived by the body [15].

When the skin is in contact with a material, material's temperature is not the only thing that determines the thermal perception. Material structural properties also plays an important role for the sensation of an object. This is because thermal sensation is directly related with the amount of heat extracted from the dermis. As stated in the introduction amount of heat flux conducted to the material determines the perception. The heat flux between an object and the

human skin can be defined by using semi-infinite model [1, 4]. Jones et al used this model to develop thermal displays. They assumed that the body and the object are semi-infinite bodies. It is assumed that in their model the contact time is quite brief so that blood circulation in the point of touch does keep the temperature of the skin constant, it is time dependent ($T_{skin,i}$). Therefore the equilibrium temperature at the point of contact (T_s) is lower than the skin temperature and the higher than the object's temperature. The analytical solution of this model leads to equation 2.1.1.[1]

$$q''_{skin} = \frac{k_{skin}(T_s - T_{skin,i})}{(\pi \alpha_{skin} t)^{\frac{1}{2}}} \quad (2.1.1)$$

Sarda et al investigates heat perception of people when they touch to the different car compartments [16]. The measurements of Sarda et al. goes beyond the previous studies because they try to mimic human skin using layers of materials with the thermoreceptors embedded. Artificial human finger is prepared by coating of latex and rubber on top of aluminum alloy A3G. Rubber and latex were chosen because their thermal properties most resemble with the thermal properties of skin. Thermoreaders lays 1 mm under the coating to make the measurements similar to the physiological system. To evaluate the heat transfer, Sarde et al. also use the transient heat of conduction equation. The equation is solved in one dimensional (1D) space and two dimensional (2D) space. The temperature solutions for 1D and 2D equations differ only in the range of 0.01°C. Therefore they concluded that solving 1D transient heat of conduction is sufficient to evaluate the sensation of warmness or coldness.

2.2 Aerogels

Aerogels are nanoporous materials which was first introduced to the literature by Kistler [17]. They are obtained from gels in which the liquid is replaced by air without the destruction of the gel solid structure. The substitution of the liquid with air is achieved by supercritical drying

technique. The maintaining the original solid structure of the gels gives aerogels distinctive properties such as exceptionally high porosity , high specific surface area and low thermal conductivity . The pore size of aerogels lays in the mesoporous range. The synthesis of aerogels can be summarized in four steps; forming the gel through polymerization reaction, aging the gel, replacing the liquid in the pores of the gel with a liquid which has a high miscibility in the desired supercritical fluid and drying the gel with supercritical fluid. The structural properties of aerogels can be manipulated changing gel synthesis parameters. Organic and inorganic aerogels can be synthesized by changing the material composition of the gel's solid structure. Organic aerogels can be synthesized using resorcinol formaldehyde, melamine formaldehyde, alginate, wheat and many more. Titania aerogels and silica aerogels are the some examples for inorganic aerogels.

2.2.1 Synthesis of Resorcinol Formaldehyde Aerogel

Resorcinol formaldehyde aerogels (RFAs) were first synthesized by Pekala by the polycondensation reaction of resorcinol (R) and formaldehyde (F) [18]. RFAs possess a porosity usually more than 80% and their specific surface area is in the range of 400-1200 m^2/g. One distinctive property of RFAs is their low thermal conductivity. Thermal conductivity of RFA can be as low as 12 mW/mK [8].

The first step of RFA synthesis is to synthesize a resorcinol formaldehyde gel a. To form the gel firstly, resorcinol is dissolved in a liquid medium. Usually a basic catalyst is used in the addition reaction of resorcinol and formaldehyde. Reaction without the catalyst is also possible. Most commonly used solvent for the reaction is water and sodium carbonate (Na_2CO_3) is the typical catalyst. Slightly acidic alkaline solutions and dilute acids or dilute bases are also used in some studies to investigate the pH effect on the gel structure. At very acidic concentrations precipitation of reactants are observed. Acidic conditions also leads to gels with wide pore size distribution. Changing the pH is a way to tune the particle size in the polymer chain. The resorcinol molecule is capable to add formaldehyde to its aromatic ring at the positions 2,4 and/or

6. Addition of Na_2CO_3 promotes hydrogen abstraction from the resorcinol molecule. This plays crucial role in the addition reaction of resorcinol and formaldehyde [8, 19]. Once the deprotonation of resorcinol occurs, formaldehyde starts to react to form an intermediate molecule with hydroxyl methyl groups.

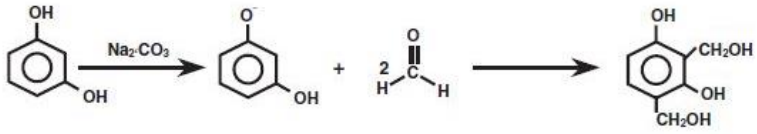

Figure 2-1: Deprotonation of resorcinol and addition reaction [8]

Deprotonation of the resorcinol molecule increases the acidity of the reaction media. The intermediate molecules starts to form methylene and methylene ether bridges between themselves and this starts the condensation reaction. These bridges are formed in the acidic medium. As the more and more links are formed between the molecules clusters of polymer stats to form. Clusters are further linked with each other to form the wet gel at the end. The gel prepared at this step is called hydrogel since it has water inside the pores.

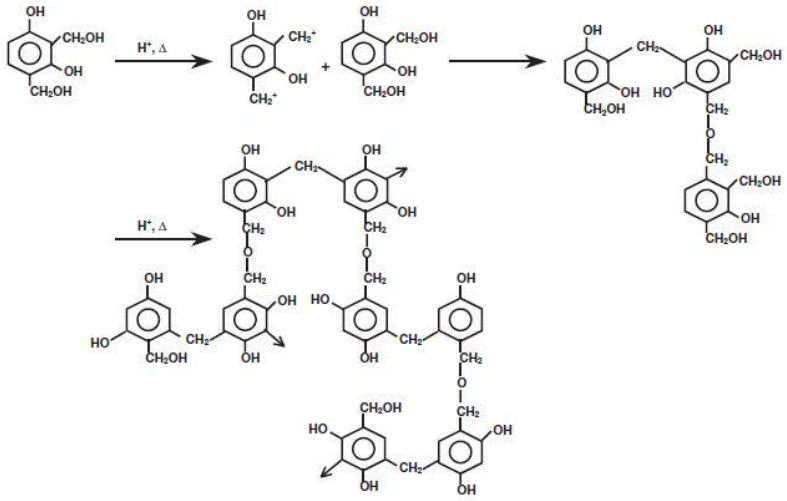

Figure 2-2: The final part of multi-step condensation reaction [8]

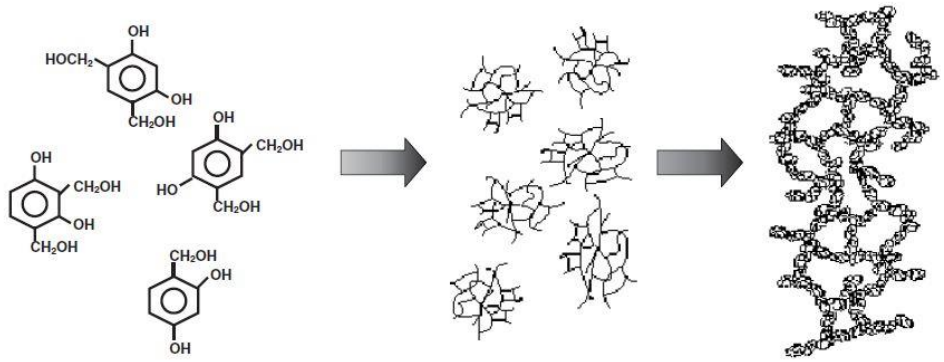

Figure 2-3: Cluster growth and formation of gel for RFAs [8]

The overall multi-step condensation reaction is an endothermic reaction. In order to form a gel with well linked clusters, gels are cured. The complete gel structure is usually obtained after curing. The complete gel formation can be also achieved at room temperature. However due to slow reaction kinetic at lower temperatures it takes weeks to obtain a rigid gel structure. Therefore after the reactants are mixed for several minutes, solution is poured into sealed molds. The usually time for the curing is about 3 days and the temperature around 80°C is used. The time of curing the gel can be shorten by a different choice of solvent during the synthesis part. For example using acetone in the reaction medium decreases the curing temperature to 40°C. The gelation time also depends on the ratios of resorcinol and the catalyst. The low R to C ratio gelation decreases the gelation time to 24 hours [8].

Once the gel is cured, a rigid structure with the shape of the mold is obtained. The solvent exchange step is performed to prepare the gels for the supercritical drying. The solvent to replace water in the gel is chosen such that it has a high miscibility in the supercritical CO_2. Acetone is usually used at this step. However other supercritical CO_2 soluble solvent can be also used. The gels are placed in acetone for several days to make sure the liquid content of the gel is completely consists of acetone. The acetone is replaced with the new one frequently to achieve this purpose. After the solvent exchange step the liquid is replaced by air using supercritical drying [18].

The most critical step to obtain aerogels is performing the supercritical drying. If the gels are exposed to air prior to supercritical drying, air liquid interface forms in the pores. The interfacial tension during the evaporation leads to the collapse of the pores. The capillary pressure inside the pores during evaporation can be up to 100 MPa. The gels which are exposed to ambient drying are called xerogels. Their structural properties are similar to the resin form of the material which they are made from. They have low porosity and high density. Using supercritical fluids suppress the formation of interfacial tension. The liquid in the pores is removed without collapsing the pore structure. The temperature and pressure is above the two phase region on the binary phase diagram of CO_2 and the acetone. The phase separation of these fluid occur at the exit of the vessel. The drying time of the gels depends on the shape and the amount of the gels. It is also reported by Czakkel et al. that the process of depressurization has an effect on the gel structure. The fast release from the vessel can also lead to the destruction of the pores.

The RFA synthesis is summarized in the figure below.

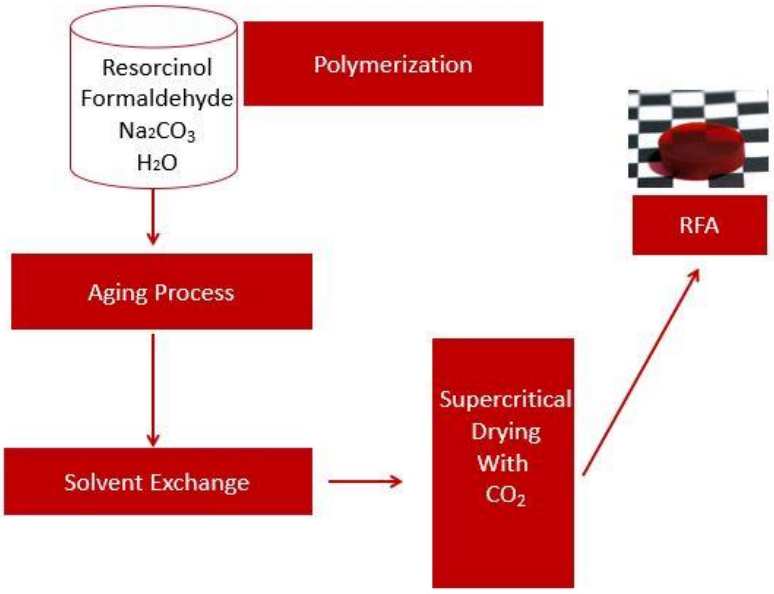

Figure 2-4: RFA synthesis summary

2.2.2 Synthesis of Silica Aerogels

Silica aerogels (SAs) are one of most studied aerogels in the literature. The development of silica aerogels dates. They are synthesized through a sol-gel route which was developed early 1960s [20]. As a silica source tetraethyl orthosilicate (TEOS), tetramethoxysilane (TMOS), methyltriethoxysilane MTES and methyltrimethoxysilane (MTMS) are commonly used. These metallic precursors contain the silica atom in the middle of structure and the difference between them is the different attached organic groups. TEOS was used in this study and the silica aerogel derived from TEOS will be discussed. The first step involves dissolving the TEOS in a liquid medium. Ethanol is usually used to create homogenous medium for the TEOS and water mixture. Increasing TEOS amount increases the density of the gel. However the percent silica that would be obtained at the end is limited by the ternary phase diagram of TEOS, water and ethanol.

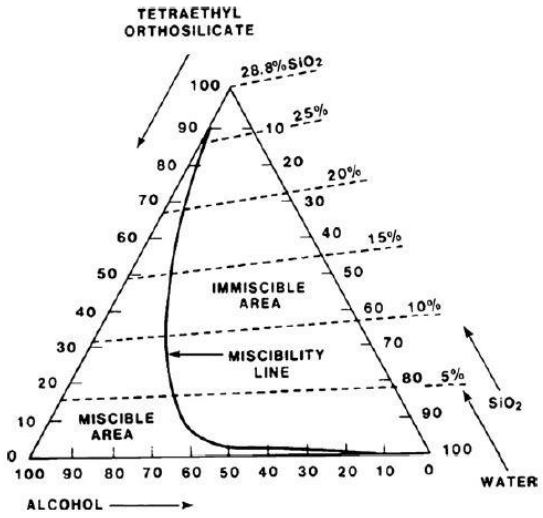

Figure 2-5: Ternary phase diagram of TEOS, water and ethanol

The synthesis of SA starts with the hydrolysis step in which alkoxide groups of TEOS replaced with hydroxyl groups. Hydrolysis reaction is shown in 2.2.2.1. Usually an acid catalyst is utilized to increase the hydrolysis reaction rate. The typical choice of acid catalyst is

hydrochloric acid (HCl). The condensation reaction occurs simultaneously with the hydrolysis reaction. Condensation reaction is a polymerization reaction in which the siloxane bonds. The rate of condensation reaction can be enhanced by using a base catalyst. A common catalyst is NH_4OH. The condensation reaction have alcohol and water as the products [9].

$$Si(OR)_4 + H_2O \leftrightarrow Si(OH)_4 + H_2O \quad (2.2.2.1)$$

$$\equiv Si - OH + OH - Si \leftrightarrow \equiv Si - O - Si \equiv + H_2O \quad (2.2.2.2)$$

$$\equiv Si - OH + RO - Si \leftrightarrow \equiv Si - O - Si \equiv + ROH \quad (2.2.2.3)$$

As these three reactions simultaneously occur at the end very long chains of silica polymers which are entangled to each other is obtained. The overall reaction is shown below.

$$n[Si(OR)_4 + Si(OR)_4] \leftrightarrow n[(OH)_3Si - Si(OH)_3] + 2\,nH_2O \quad (2.2.2.4)$$

When the all the reactants and catalyst are added, even if an observable solid gel structure forms, there can be still unhydrolized precursors in the medium. To fasten the process further resulting gels are usually cured at 50°C in ethanol-water solution. The native solution of TEOS, ethanol and water can be also used at the aging step to form additional new bonds. Creation of new bonds increases the mechanical strength of the gels. Also during the aging process shrinkage occurs. Aging process is thoroughly studied in the literature to obtain crack free and mechanically strong aerogels.

The pores of the resulting gel contains alcohol and other impurities in the pores. Therefore solvent exchange step is applied. The majority of pores are occupied by ethanol. Therefore at the solvent exchange step, gels are washed with ethanol several times. The solubility of ethanol in supercritical water is high. Supercritical drying is applied to obtain SAs. The summary of silica aerogel production is presented in the below figure.

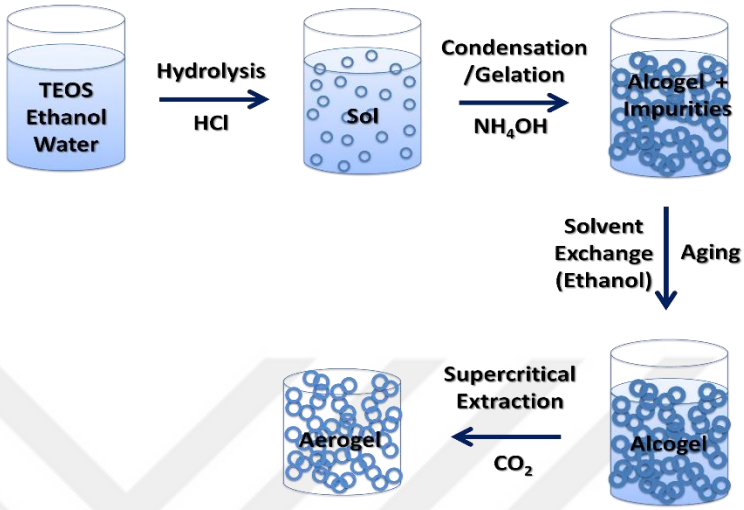

[21]

Figure 2-6: Silica aerogel synthesis process

2.2.3 Thermal Properties of Aerogels

One of the distinctive properties of aerogels is their excellent thermal insulation property compared to the insulation materials currently used in the industry. The heat transfer through the porous medium of the aerogels are not as simple as the materials with a single phase. Aerogels have solid skeleton and pores with gaseous. When there is a heat flow across the aerogel, heat has to pass through the solid skeleton and the pores. Therefore different heat transfer modes are involved in aerogels and the schematic representation is given in the Figure 2.7; heat transfer through the solid-backbone (brown lines), heat transfer through the gaseous phase (blue lines) and heat transfer by radiation (red lines). Heat transfer by radiation exists for every object and it due to the thermal agitation which exist for materials above 0 K. Even though the heat transfer modes are written, the coupling effect between these modes exists. Thermal properties of aerogels strongly depend on the structure of the aerogel. If one structural property, such as pore volume of aerogel, changes, it would have an effect all the heat transfer modes. The main component of the heat transfer is the thermal conductivity. Therefore the relation between the

structure of the aerogel and its effect on the thermal conductivity each heat transfer mode is studied.[22, 23]

$$k_{effective} = k_{solid} + k_{gaseous} + k_{radiative} \quad (2.2.3)$$

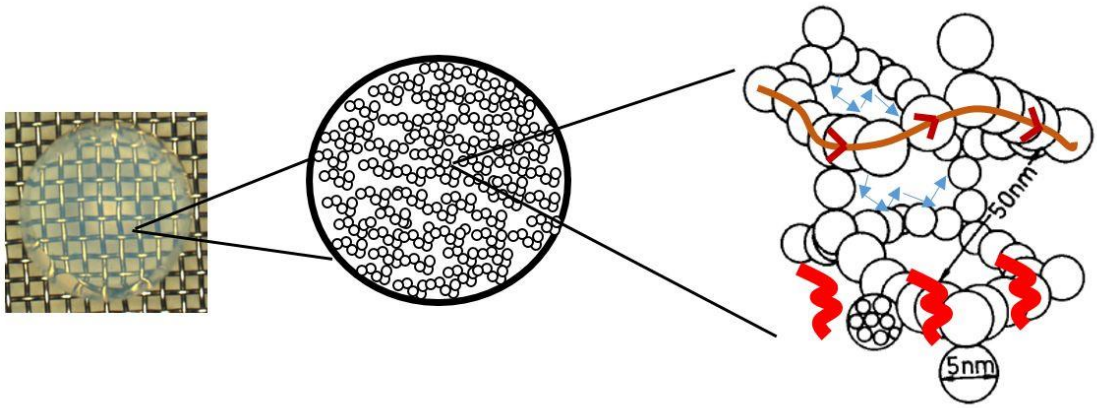

Figure 2-7: Schematic view of heat transfer modes in an aerogels

2.2.3.1 Solid Thermal Conductivity in Aerogels

One of the reasons that aerogels have very low thermal conductivity is that their solid thermal conductivity is reduced compared to the thermal conductivity of the solid which makes the solid backbone structure. For example silica aerogel's solid backbone thermal conductivity can be nearly reduced by 1000 times compared to the thermal conductivity of fused silica [23]. The solid backbone density of an aerogel depends on the material composition, density and the backbone connectivity. The polymer chains meander across the whole structures and some are in contact with each other with small necks. The ineffective dead ends are also present in the structure. The entangled chains and the small neck connections between them suppressed the heat flow. Heat is transferred by the phonons through the solid part. The fundamentals of solid thermal conductivity comes from the phonon diffusion model. The model relates the solid thermal conductivity with the mean free path of phonons, specific heat capacity, bulk density and sound

velocity across the backbone. The phonon diffusion model's outcome is combined with the geometric factor to give a rather simplistic equation for the solid thermal conductivity [24].

$$k_{solid,aerogel} = k_0 \times \frac{\rho_{aerogel}}{\rho_{solid}} \times \frac{v_{aerogel}}{v_{solid}} \quad (2.2.3.3.1)$$

where, $\rho_{aerogel}$ is the bulk density of aerogel, ρ_{solid} is the density of the native solid material which makes the backbone, $v_{aerogel}$ is the longitudinal sound velocity through aerogel and v_{solid} longitudinal sound velocity through the native material. This equation shows that aerogel's bulk density is the most influential structural property that effects the solid thermal conductivity. As the density of an aerogel decreases the solid content is also decreased. Lu et. al. also examined the density dependence on thermal conductivity for monolithic resorcinol formaldehyde aerogels in the density range of 70 to 230 kg/m^3 and they have found that the solid thermal conductivity approximately proportional to the 1.5 power of density. Therefore even a small change in the bulk density can show a vast amount of change in the solid thermal conductivity.

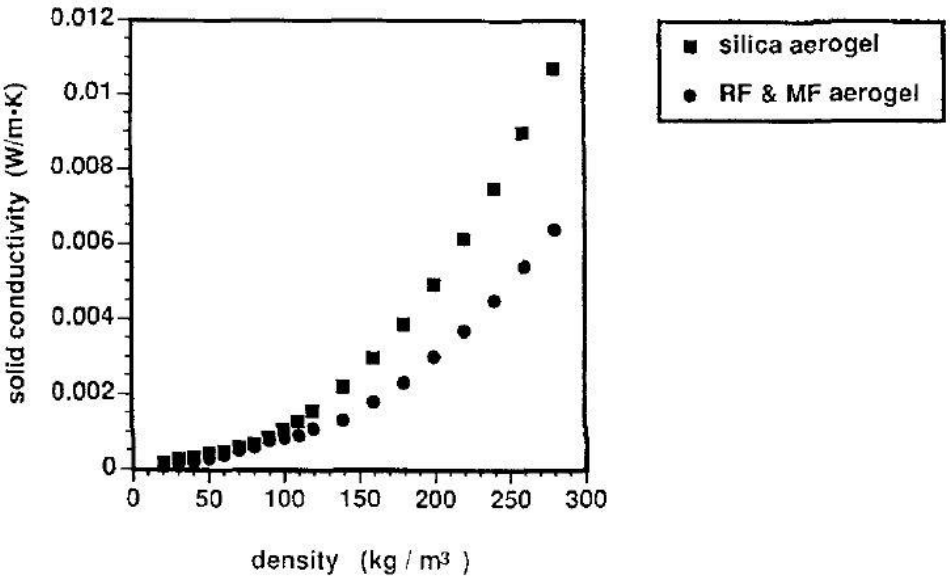

[24]

Figure 2-8: Effect of density on the solid thermal conductivity

The biggest portion of the effective thermal conductivity comes from the solid thermal conductivity. In summary, density is the major structural property that changes the solid thermal

conductivity. As shown on the Figure 2-8, exponential increase with the density observed. Therefore in order to obtain aerogels with low thermal conductivity, the density should be as minimum as possible. However there is a trade of between the density and the mechanical strength of the aerogel. Therefore usually aerogels with very low densities are not suitable for industrial application.

2.2.3.2 Gaseous Thermal Conductivity

Since the porosity of aerogels are is quite large, the heat transfer through the gas phase is another important mode that has an effect on the overall thermal conductivity of aerogels. As stated earlier, pore size of aerogels in the mesopore range. Since the mean free path of air molecules in ambient conditions quite larger than the pores, convective heat transfer is suppressed in aerogels. Knudson number (Kn) can be used to describe the heat transfer mode of air molecules in the pores of aerogel. It is a ratio of mean free path of a gas molecule (l_g) to the pore diameter(D). [22-25]

$$Kn = \frac{l_g}{D} \quad (2.2.3.4.1)$$

Molecular heat transfer becomes dominant for the porous system which have Knudson number larger than 1. In such system the gas molecules mainly collide with walls of the aerogel skeleton. The number of collisions between the air molecules is less than the number of collision with the wall. This is called the Knudson flow and the thermal conductivity is suppressed. For Knudson numbers which have value smaller than one, the air molecules mainly collide with each other. In that case air molecules flow easily like a liquid inside the pores. Thermal conductivity of gaseous phase is equal or close the thermal conductivity of air at ambient conditions. The Knudson number near 1 gives a heat transfer mode which is a combination of molecular and diffusive heat transfer. The gas molecules collide with the same frequency with each other and with the wall of the backbone. Other than the pore size of the aerogel structure, gaseous thermal conductivity depends on the type of gas in the pores, number of the gas molecules in the structure (pressure) and the porosity. Fricke et al. reported following empirical equation to predict the gaseous thermal conductivity of aerogels[23];

$$k_{gas} = \frac{k_0 \emptyset}{1+2\beta Kn} \quad (2.2.3.4.2)$$

where k_0 is the thermal conductivity of the gas which occupies the pores, $\emptyset$ is the porosity, Kn is the Knudson number and β is a constant which includes the energy transfer between the gas molecules in a constrained solid structure. β for air containing aerogels is usually around 2.

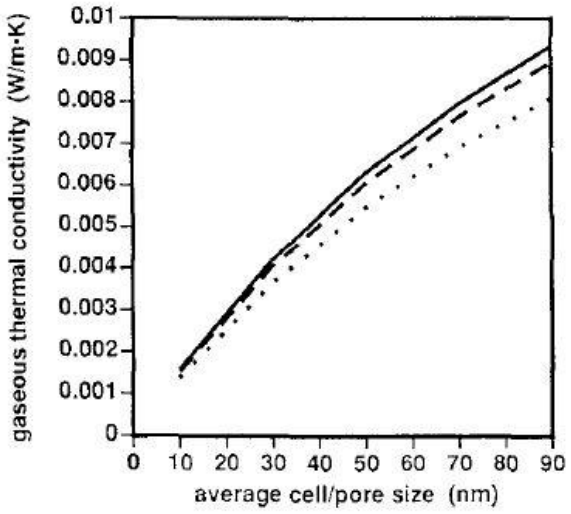

[22]

Figure 2-9: Gaseous thermal conductivity's dependence on the pores size

In summary the gaseous thermal conductivity depends mostly on the pore volume. Aerogels' with very low pore volume or pore diameter has a very low gaseous thermal conductivity. Porosity defines the volume fraction of gas in the overall structure. Bulk density is directly related with the porosity. As stated earlier not a single but almost all structural properties have an effect on the each heat transfer form.

2.2.3.3 Radiative thermal conductivity

Radiative heat transfer becomes significant only at higher temperatures for the most materials. Radiative heat transfer occurs by the movement of photons. The frequency of photon interactions with the backbone determines the magnitude of the radiative heat transfer. Optical thickness is a measure of this interaction. Most of the solid materials are optically thick. Therefore their radiative thermal conductivity is negligible. Whereas optical thickness for the most porous material is low. As for the aerogels; most organic aerogels exhibit high optically thickness. For the optically thick porous materials Rosseland approximation is used to formulate the radiative thermal conductivity [23, 26-28];

$$k_r = \frac{16n^2\sigma T_r^3}{3\rho\, e(T)} \quad (2.2.3.5.1)$$

Where n is the refractive index for the aerogel (usually close to 1), σ is the Stephan-Boltzman constant, T_r is the critical temperature, ρ is the aerogel bulk density and $e(T)$ is the extinction coefficient.

Table 1: Extinction coefficient for various materials

Compound	Specific Extinction Coefficient
SA	22.7
SA (opacified)	84.2
TiO_2 Aerogel	32.6
Carbon	>1000
RFA	50.1
Polystyrene	47.6

Extinction coefficients for various materials are presented in Table 1. The aerogels reported in the table have a low density. SAs has a low specific extinction coefficient compared to RFAs.

Opacifiers are used to decrease the specific extinction coefficient. If an aerogel possess relatively high density, then its radiative thermal conductivity can be ignored. The value for the radiative thermal conductivity at room temperature is usually around 4 mW/mK. Therefore its contribution to the overall effective thermal conductivity can be negligible depending on the density.

2.2.3.4 Effective thermal conductivity of an aerogel

As stated in the beginning of Section 2.2.3 the effective thermal conductivity of an aerogel is the summation of solid, gaseous and radiative thermal conductivity. One must not forget that most of the thermal conductivity equations presented in this section empirical equations. Also models and assumption are used to predict the experimental data. All equation are connected to each other. However for the simplicity and to get a good understanding of what happens in each heat transfer mode, the terms are arranged such that they can be called solid, gaseous and radiative thermal conductivity. The models and equations mostly coincide well with the experimental data. The contribution of individual thermal conductivity on the effective thermal conductivity is shown in the figure below [22].

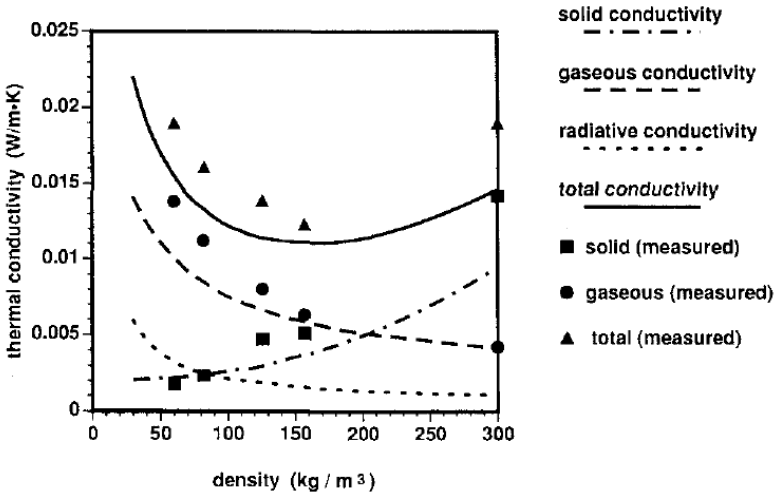

Figure 2-10: Effective Thermal Conductivity with each transfer mode

2.3 Urea Formaldehyde Polymer

Urea formaldehyde (UF) is a thermos setting polymer which is commonly used for the production of adhesives, additives in fiberboards and molded objects [29]. It has a mechanical strength, low water absorptivity and low mold shrinkage value. It is produced through a condensation reaction in which urea and formaldehyde react with the usage of base and heat (Figure 2-11).

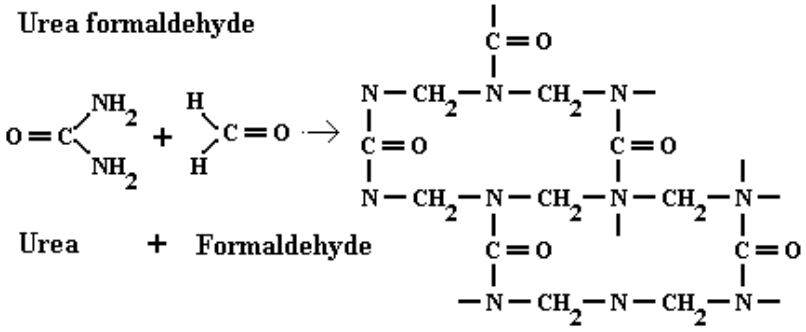

Figure 2-11: Synthesis of urea formaldehyde polymer

Urea formaldehyde molecules for molding are produced in a granular form with the usage of extruder. The grains of UF requires heat and pressure to complete the linkage between the UF clusters. In the grain form, UF has a high water absorptivity and it can be decompose under sunlight and with humidity. The reaction only reaches to completion at the end of hot pressing. Usually pressure around 100 Bars and temperatures around 140°C are needed to form rigid plate form of UF. Material properties of UF are summarized in Table 2.

Table 2: Material Properties of UF

Material Property	
Density	1.5 g/cm^3
Thermal Conductivity	480 mW/mK
Heat Capacity	1200 J/kg.K
Tensile Strength	30 MPa

2.4 Composites of Aerogels

Aerogel composites are studies to add new functions native structure and to modify and improve the existing property of aerogels. In the literature most studies focus on the improvement of mechanical strength of aerogels. Organic or inorganic polymers can be incorporated into the structure before gelation, reacting the polymer with the surface groups of the aerogel or the polymer can be added during the reaction [21, 30]. Mechanical properties of aerogels are usually enhanced by the polymer addition. However the thermal properties of resulting composites are not as good as the native aerogels. Composites of biodegradable aerogels are also being used for the controlled drug delivery purposes [31]. These composites are created so that mass transfer between the layers of aerogel can be manipulated. The studies on aerogel composites are usually formed by bringing the aerogel and the polymer during synthesis or after synthesis through reactions. This is not possible with the UF used in this study. To the best of knowledge, there is there is no urea-formaldehyde and aerogel composite present in the literature.

There very limited studies in the literature which makes the aerogel composites of polymers that have similar manufacture properties with the UF. Polytetrafluoroethylene (PTFE) based aerogel composites are manufactured. Ristic-Lehmann et al. propose in their patent to manufacturing a composite which contains layers of the silica aerogels and PTFE to make flexible sheet which has a possible application as a blanket [32]. A dispersion containing commercial hydrophobic silica aerogels is mixed with an aqueous solution containing dispersed polytetrafluoroethylene (PTFE). With the addition of solvents and surfactants, the mixture coagulate. Then the coagulated mixture is dried and cake of PTFE and silica aerogels is obtained. The final form of the composite was obtained after drying and pressing the dried cake around 3 bars.

2.5 Mathematical models to predict the effective thermal conductivity of Composites

Effective thermal conductivity calculation strategies are based on heterogeneous material's electrical conductivity, permittivity and permeability calculations. These methodologies to

calculate the effective thermal conductivity, date back to the Maxwell's studies in 19th century [33, 34]. Maxwell solved the electrical potential of a spherical particle in an infinitely expanded homogenously medium. Then he calculated the background potential associated with the singles sphere in medium filled with n numbers of sphere. The effective electrical resistivity was obtained by considering the interaction between spheres. Effective electrical resistivity was related with the thermal conductivity by inverse relation. Maxwell model is a simple and effective model. Thermal conductivity and volume fraction of the materials which make up the object are the required data for the calculation of effective thermal conductivity. Maxwell model works for the composite system with the dilute fillers. Other models modify the Maxwell to predict the composites with high filler concentrations. Maxwell model and other models for predicting effective thermal conductivity are discussed in the sections below.

2.5.1 Maxwell Model

Maxwell model assumes a dilute dispersion of non-interacting spherical particles (fillers) in continuous media. The model considers low concentration of spherical materials (less than 25 vol% of filler particles) which have a thermal conductivity of k_1 dispersed in a continuous medium with a thermal conductivity of k_m[35, 36].

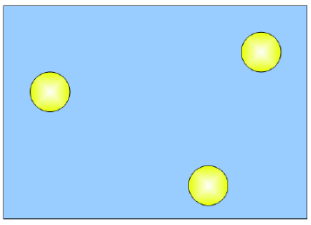

Figure 2-12: Maxwell Model

$$\frac{k_{eff}}{k_m} = 1 + \frac{3\emptyset}{\left(\frac{k_1+2k_m}{k_1-k_m}\right)-\emptyset} \quad (2.5.1.1)$$

where $\emptyset$ is the volume fraction of the filler.

Eucken modified the Maxwell equation to be used slightly higher filler concentrations. The modified equation is called Maxwell-Eucken equation. Two forms of the equation exists depending on which component is chosen to be the filler or the continuous phase. K represents the effective thermal conductivity of the structure. In Figure 2-13, the model on the left is ME1 in which k_1 is the thermal conductivity of continuous phase and k_2 is the thermal conductivity of

dispersed phase. *V* is the volume fraction of each compound. The model on the right is the ME-2. In this model the parameters with 1 indices belong to the material in the continuous phase[36].

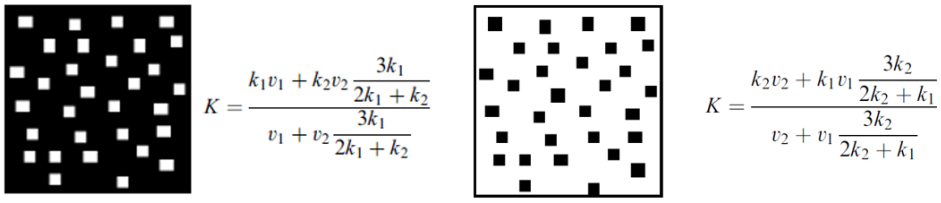

Figure 2-13: Maxwell Eucken equation

2.5.2 Rayleigh's Model

Rayleigh also considered spherical particles dispersed in a continuous medium. The arrangement of these spheres were in a simple cubic fashion. The difference from the Maxwell's model is that Rayleigh included the effect of interaction between these dispersed spheres. At higher filler concentration in the medium, effect of interactions between the filler materials cannot be neglected. Therefore at high volumetric concentrations Rayleigh's model gives more accurate result. The interaction terms in the equation are in the denominator as high order series. As the volume fraction approaches to 0, Rayleigh' solution becomes Maxwell equation[33].

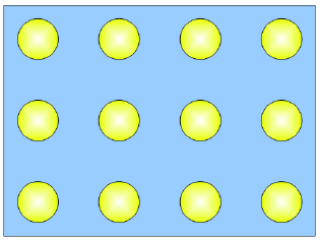

Figure 2-14: Simple cubic arrangement of fillers

$$\frac{k_{eff}}{k_m} = 1 + \frac{3\emptyset}{\left(\frac{k_1+2k_m}{k_1-k_m}\right) - \emptyset + 1.569\left(\frac{k_1-k_m}{3k_1-4k_m}\right)\emptyset^{\frac{10}{3}} + \cdots}$$

Rayleigh expanded his solution for the system of the cylinders laying in a composite matrix. The existence of these fibers makes the effective thermal conductivity directional.

2.5.3 Levy's Model

Levy modified the Maxwell-Eucken equation to get rid of the problem of choosing which form of the Maxwell-Eucken equation to use. The model was constructed merely by the algebraic manipulation of the two forms of Maxwell-Eucken equations. Model's applicability to food composites were proven by Pham and Willix [37]. However they stated that even the model works quite well with the experimental data, the model lacks necessary physical justification. Levy's model was justified by the Wang et al. in their article where they attempted to come up with a unifying equation for the effective thermal conductivity models. Levy's model gave identical results with the Wang's model where he combined both of the Maxwell-Eucken models by taking the equal volume of both models in a homogenous matrix Figure 2-15 [36].

$$K = k_m \frac{2k_m + k_1 - 2(k_m - k_1)F}{2k_m + k_1 + (k_m - k_1)F} \quad (2.5.3.1)$$

$$F = \frac{{}^{2}/_{G} - 1 + 2\vartheta_1 - \sqrt{({}^{2}/_{G} - 1 + 2\vartheta_1)^2 - {}^{8\vartheta_1}/_{G}}}{2} \quad (2.5.3.2)$$

$$G = \frac{(k_m - k_1)^2}{(k_m + k_1)^2 + {}^{k_m k_1}/_{2}} \quad (2.5.3.3)$$

where, ϑ_1 is the volume fraction of dispersed phase, F and G are the constants for the Levy's model, thermal conductivity of k_1 dispersed in a continuous medium with a thermal conductivity of k_m.

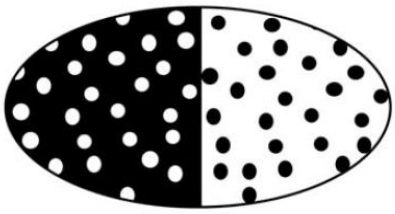

Figure 2-15: EM-1 and EM-2 equal volume model

2.5.4 Effective Medium Theory (EMT)

This model is also first developed to predict the electrical properties of particles. Completely random distribution of particles are considered in this model. Mean field theory is applied to find the effective thermal conductivity. In mean field theory macroscopic properties are predicted by using stochastic models which predict the properties of small portion of the randomly distributed materials [38]. EMT assumes that the composite is homogeneous in macroscopic scale. The drawback of EMT is their completely inaccurate predictions beyond certain volume fractions due to the model's assumptions. The volume fraction where the prediction of EMT does not hold is called percolation threshold [36]. This phenomena occurs when there is appreciably difference exists between the materials which constitute the composite. As the filler compound gets closer to the each other, they produce a gate way where the overall property of the composite can be hugely depend on this region. Therefore in the composite properties such as electrical conductivity and thermal conductivity sudden changes are expected [36]. However compared to other models EMT predicts the effective thermal conductivity better at high filler concentrations which is below the percolation threshold.

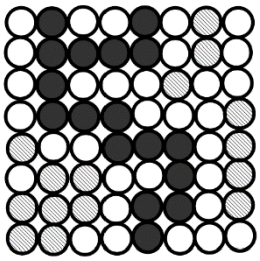

Figure 2-17: Percolation phenomena observed when the filler (black) particles are in contact

$$v_1 \frac{k_1 - K}{k_1 + 2K} + v_2 \frac{k_2 - K}{k_2 + 2K} = 0$$

Figure 2-16: EMT Model

In Figure 2-16, K is the effective thermal conductivity. k_i and v_i are thermal conductivity and volume fraction respectively.

Chapter 3 Experimental Procedure and Characterization Techniques

3.1 Materials

Sodium carbonate (99.99%) was purchased from Merck. Formaldehyde (37% stabilized in 10% methanol) was purchased from VWR. Resorcinol (≥99%), Ethanol (99.9%), TEOS (98.0 %) and ammonium hydroxide (NH_4OH) (2.0 M in ethanol) were purchased from Sigma Aldrich. Acetone (technical grade) was purchased from Onur Kimya. Hydrochloric acid (HCl 37%) was obtained from Riedel-de Haën. Urea formaldehyde was purchased in granular form from Körfez Kimya. Carbon dioxide (99.998%), Helium (99.999%), Nitrogen (99.99%) was purchased from Air Liquide.

3.2 Synthesis of Aerogels Resorcinol Formaldehyde Aerogels

Resorcinol formaldehyde aerogels were synthesized based on the polycondensation procedure described by Pekala [18]. Resorcinol (R) was first dissolved in water (W). The solution were mixed for approximately 5 minutes to make sure that all R dissolves. Sodium carbonate (C) was then added into the solution and the mixture was stirred for another 5 minutes. Then the formaldehyde is added into the mixture. R:F ratios were kept constant for the resorcinol formaldehyde gels with different densities. R:C and R:W was changed. Dense RFAs obtained were denoted by RFA-H, and relatively less dense RFAs just denoted as RFA.

Table 3: Ratios of the reactants and amount of reactants used for the RFA synthesis

R/C=200	**R/F**=0.50 (0.46)*	**R/W**=0.02

*Excess formaldehyde is provided

Chemical	**Amounts Used**	
Resorcinol	0.078 moles	8.5645 grams
Water	3.885 moles	70 grams
Na_2CO_3 (anhydrous)	3.897×10^{-4} moles	0.0413 grams
Formaldehyde	0.1683 moles	12.96 mL**

**from the stock solution (37%)

Table 4: Ratios of the reactants and amount of reactants used for the RFA-H synthesis

R/C=50	**R/F**=0.50 *	**R/W**=0.08

*Excess formaldehyde is provided

Chemical	**Amounts Used**	
Resorcinol	0.078 moles	8.5645 grams
Water	0.975 moles	17.57 grams
Na_2CO_3 (anhydrous)	1.56 x 10^{-3} moles	0.1653 grams
Formaldehyde	0.1683 moles	12.96 mL**

*from the stock solution (37%)

Even though one mole of R reacts with two moles of F, excess amount of F is provided to make sure that all of the R in the medium goes into the reaction. After formaldehyde addition the mixture was stirred for 3 more minutes and then solution were poured into the polypropylene molds and the molds were sealed. They were cured at room temperature for one day, at 50°C for another 24 hours and at 90°C for three days. Then the seals of the mold were broken and the gels were immediately placed in technical grade acetone. The gels were washed with the fresh acetone every day and this procedure was repeated at least 4 days. Then the gels were dried using super critical carbon dioxide drying. The extraction was performed at 45°C and at 100 bars and details of the equipment are discussed in the section 3.3.

3.3 Synthesis of Silica Aerogels

Silica aerogels were synthesized using a two-step sol-gel procedure. TEOS was used as the silica source. TEOS was dissolved in water with ethanol (E) as co-solvent. As acid catalyst HCl was added into the solution and the mixture was stirred for 40 minutes. In order to accelerate the condensation NH_4OH was added as base catalyst. The molar ratios of the chemicals, TEOS: E: W: HCl: NH_4OH were as follows 1: 4.01: 2.97: 0.0022: 0.0089. After the addition of the base catalyst, solution was stirred for several other minutes then it was poured into molds and the molds were sealed. Once the gel structure was obtained, gels were removed from their molds and placed in ethanol-water (1:1 volume ratio) solution which was kept in 50°C oven for 24 hours.

Then solution which contains the gels were allowed to cool down to room temperature. The EtOH-Water solution was replaced by the pure EtOH. Ethanol was replaced with the fresh one for every day and this was repeated for four days. This procedure allows to produce SAs with relatively low densities in this thesis. In order to synthesize relatively high density silica aerogels (SA-H), gels were replaced into an aging solution which contained TEOS, ethanol and water. The aging solution had the following volumetric ratios for each chemical 12:3:15 respectively. The gels were kept in this aging solution for two weeks and the aging solution was changed with a fresh one with the same volumetric ratios as before three times, on the 3rd, 6th and 9th day. The gels then replaced in a pure ethanol solution for the solvent exchange step. The ethanol in the medium was replaced with the fresh one for four times. SAs were obtained after supercritical drying at 40°C and 85 bars.

3.4 Supercritical Drying

Supercritical drying was the final step to obtain aerogels. Applied Separations Speed SFE was used for this procedure. The system was composed of 5 main parts shown in the Figure 3.1.

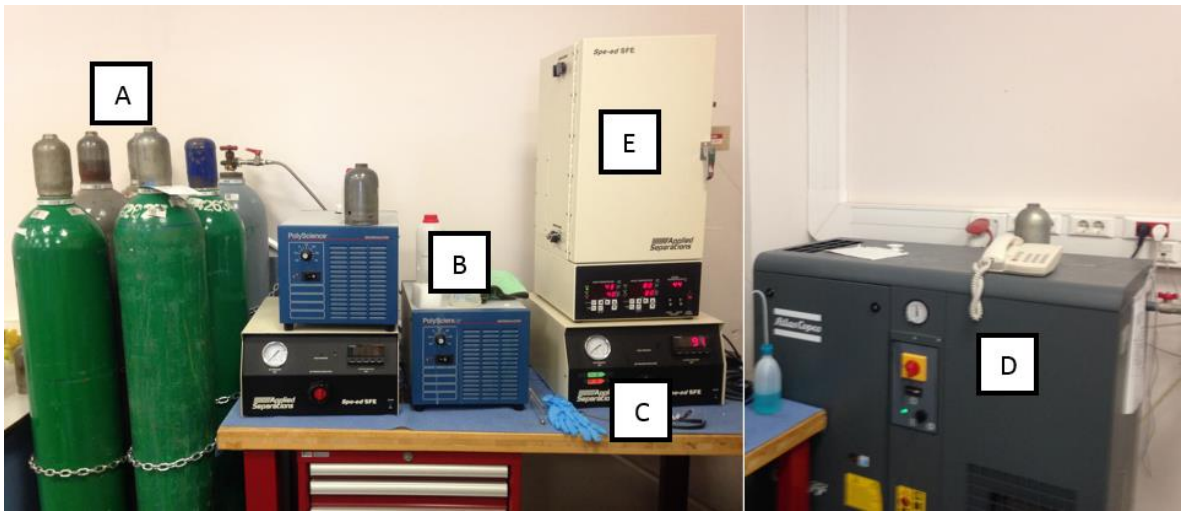

Figure 3-1: Supercritical Drying Unit

Carbon dioxide tank with siphon tube (A) supplies the high purity CO_2 (99.998%) to the system. In the tank CO_2 exists in two phase and siphon tube was used to take the liquid part of the CO_2. In order to pump CO_2 it needs to be in liquid phase. Therefore to convert the gas phase completely into liquid phase a chiller was used to cool the stream to -15°C (B). To pressurize the pump air driven pump (C) which was worked with a compressor (D) was used. The stream was then entered to the oven (E) where the temperate was raised to reach above the one phase, supercritical region of mixture of CO_2 and acetone or ethanol. A stainless steel vessel (500 mL) with the gels in the acetone or ethanol medium was used. The vessel was connected in the oven prior to the drying to make sure that it was at the operation temperature. To make sure that temperature equilibrium was sustained between the vessel, liquid and gel, the vessel was heated in an oven before night of the drying. When CO_2 was stream enters into the oven, it goes into the supercritical phase. Supercritical drying lasted at least 5 hours after bulk the ethanol or the acetone in vessel removed.

Figure 3-2: 500 mL vessel used for supercritical drying

3.6 Preparation of UF-Aerogel Composites

Resorcinol formaldehyde and silica aerogels were crushed such that their particle size matched more or less with the particle size of the urea formaldehyde grains. Then urea formaldehyde and crushed aerogels were mixed together in a plastic bag. The aim was to achieve an even distribution of aerogel particles into urea formaldehyde grains. Preparation of composites were done in the factory of the project partner, Eczacıbaşı Vitra Bozüyük factory. Industrial scale hot presses were used. Stainless steel mold was manufactured for the purposed of this study 30 cm x 30 cm dimensions. The conventional mold for the toilet seats had a rounded shape which was not suitable for the thermal conductivity measurements. Aerogel and UF grain mixture's weight was around 1400g for almost all composites. The

mixture was cured at 50°C in an oven. Mold's temperature was kept around 138°C throughout the hot press process. Grains were then pressed in the mold at various pressures (60-100 bars) for 225 seconds. Resulting rigid composites were allowed to be cooled down at room temperature for 15 minutes. The process is summarized in Figure 3-3.

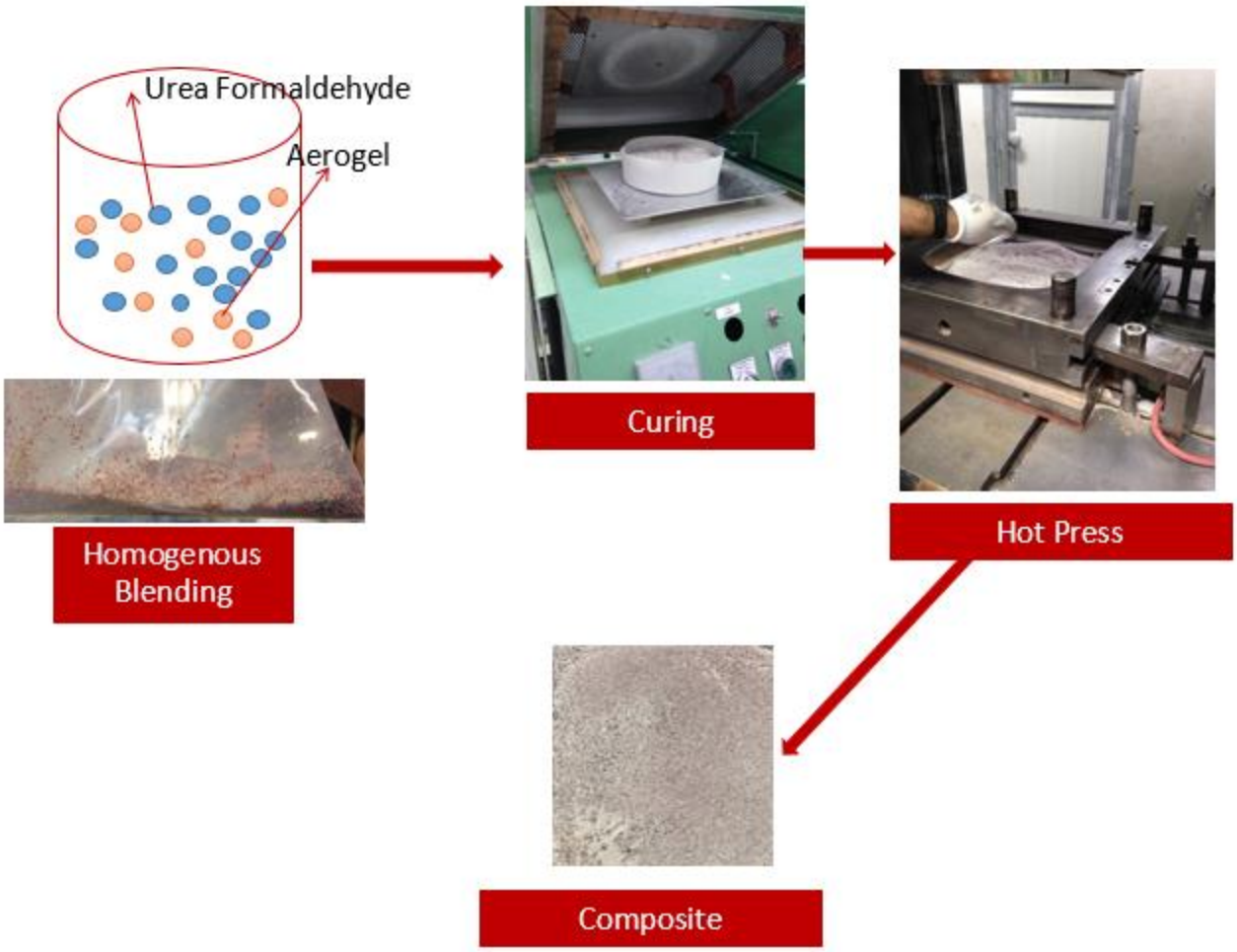

Figure 3-3: RFA-UF Composite Manufacture Flow diagram

3.6 Characterization Methods

3.6.1 Bulk Density and Porosity

One of the simple and the accurate ways of characterizing aerogels is measuring their bulk density. The measurement was done easily since the gelation was achieved in cylindrical PP molds. Molds were purchased from VWR. None of the gels did not stick on the surface of the walls; therefore RFAs and SAs were obtained in cylindrical forms. Bulk density was measured by weighing the aerogel sample and diving it by the volume. Porosity (∅) of aerogels can be calculated using the bulk density of aerogel and the solid backbone density as shown in the below equation.

Figure 3-4: VWR PP molds

$$\emptyset = \frac{\rho_{backbone} - \rho_{aerogel}}{\rho_{backbone}} \quad (3.6.1.1)$$

Pore volume (V_p) can be measured using nitrogen physisorption experiments. However it can be also estimated by using the bulk density and solid backbone density of aerogels. The assumption in this calculation is that total mass of the structure is equated to the mass of the solid backbone. This assumption is reasonable air mass can be negligible compared to the mass of solid.

$$V_p = \frac{1}{\rho_{Bulk}} - \frac{1}{\rho_{silica}} \quad (3.6.1.2)$$

Figure 3-5: Monolithic SAs obtained in PP molds

3.6.2 Nitrogen Physisorption Experiment

Micromeritics ASAP 2020 instrument was used for nitrogen physisorption experiments of aerogels. Multilayer adsorption theory was developed by Brunauer, Emmett and Teller (BET) in 1938 as an extension for the Langmuir's model of adsorption [39]. Their theory are now used to determine the surface areas and pore volume of a material. The ASAP 2020 (Figure 3-6) instrument also uses the BET theory.

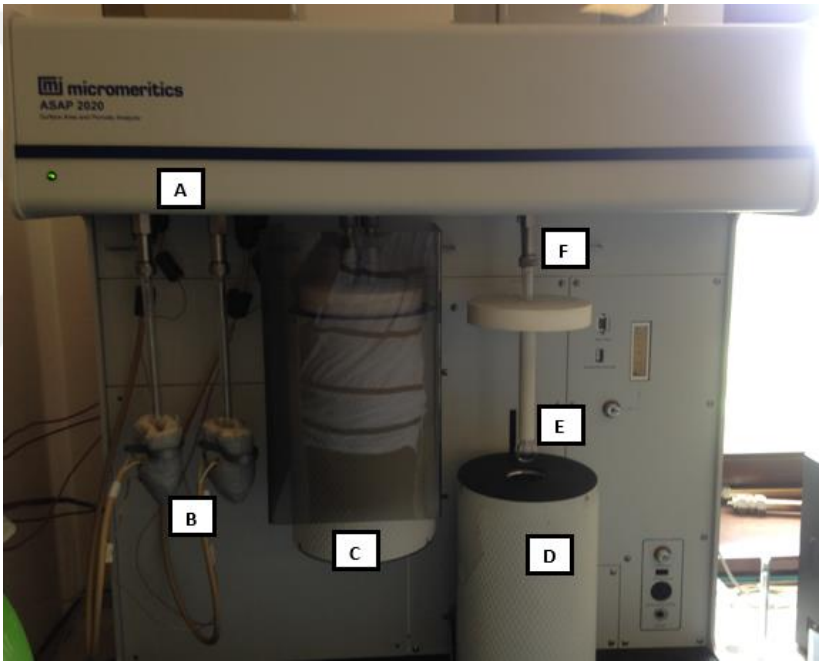

Figure 3-6: ASAP 2020 Instrument

Aerogel samples were degassed before the adsorption experiments. During degas aerogel containing glass sample tubes were connected to the degas port (A). Samples were heated and vacuum was pulled. Aerogel weight that was used during the analysis was between 100-300 mg. For RFAs degas temperature was 80°C and for SAs, it was 300°C. Heating jackets were used to maintain the elevated temperatures (B). RFAs were in degas for 24 hours and SAs were hold in degas for 3 hours. Degas was performed to remove the volatile molecules that were absorbed on the surface of aerogels. (C) is the trap where air pulled goes through. The temperature of the trap

was maintained at the temperature 77K with liquid nitrogen. Oil driven vacuum pump was used for the degas process. Traps were used to capture the impurities and any possible oil leak from the vacuum pump, so the manifold stays clean. After degas, the sample (E) were connected to the analysis port (F). Analysis was performed by increasing the nitrogen pressure in the sample tube step by step up to relative pressure of 1. Desorption was also performed for the samples. Adsorption and desorption curves were obtained at the end. Pore volume and pore size were obtained by Barrett–Joyner–Halenda (BJH) method. Surface area were determined by BET method.

3.6.3 Thermal Conductivity Measurement

Hot Disk® Thermal Constant Analyzer was used to measure the thermal conductivity of the samples. This instruments uses Transient Plane Source (TPS) method. TPS method can evaluate thermal transport properties (thermal conductivity, thermal diffusivity and heat capacity) [40, 41]. Transiently heated plane sensor was used for the measurements. This plane sensor acts both as a dynamic temperature measurement sensor and a transient heat source. Sensor was composed 10 micron of nickel double spiral which was encapsulated between an insulating material, Kapton.

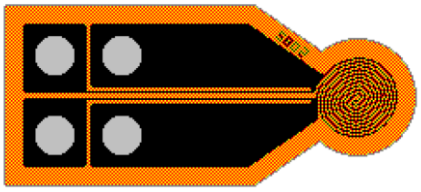

Figure 3-7: nickel-kapton based sensor

For the measurements two identical samples are needed. These samples were used to sandwich the plane sensor of the instrument. Composites were obtained in the dimensions of 30 cm x 30 cm from the mold. From this plate, 10 cm x 10 cm samples were cut. Two samples with 10 cm

x 10 cm dimensions were used to sandwich the sensor of the Hot Disk® and the measurements were conducted.

Figure 3-8: Hot Disk ® Thermal Constant Analyzer

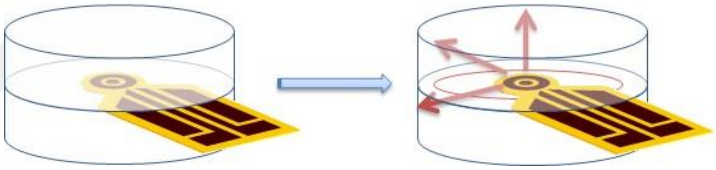

Figure 3-9: Measurement protocol of Hot Disk ®

Once the samples were place in the instrument as shown on Figure 3-9, sensor heating power and measurement time were entered to the software system. The heating power was 20 to 40 mW and the measurement time was 20 to 40 seconds for all the composites. The power and the time input were selected for each composite after making trials with various inputs until consistent results were obtained. 200 temperature measurements were collected and the results were reported. The one important thing to note about the TPS is that heat capacity is regressed from the model. Therefore accurate results for the heat capacity were not expected with this method [40, 41].

3.6.4 Heat Capacity of a Composite Material

Heat capacity of an isotopic composite material can be calculated by using the weighted average of individual specific heat capacities[42]. This calculation is valid with the experimental heat capacities of most composites including polymer composites and polymer-nanostructured material composites at moderate temperatures [43, 44].

$$c_{p,compsite} = \sum_{i=1}^{n} w_i c_{p,i}$$

Specific heat capacities (J/K.kh) of aerogels are equal to the specific heat capacity of the materials which forms the skeleton of the aerogel. The bulk density has no effect on the specific heat capacity of a material. For example, the foamed aluminum has a bulk density in the range of 0.4 to 0.9 g/cm^3. The specific heat capacity of this material is exactly equal to the specific heat capacity of dense aluminum [45]. Therefore in this thesis the heat capacities of resorcinol formaldehyde resin (840 J/K.kg) and fused silica (700 J/K.kg) were used for the aerogels made from these materials. The heat capacity of urea formaldehyde was 1200 J/K.kg [6, 29, 46].

Chapter 4 Results and Discussion

4.1 UF-RFA Composites

The first composite trial was prepared with the resorcinol formaldehyde aerogel (RFA) with a bulk density of 0.15 g/cm^3. RFAs were characterized by the techniques described in the previous chapter. The synthesized RFA's pore size was in the mesopore range with a mean value around 17 nm. The RFA with these properties was reported as the aerogel with the lowest thermal conductivity with a value of 12 mW/m.K [18].

Table 5: RFA Material Properties

Material Property	
Density	0.15 g/cm^3
Porosity	88%
BET S.A.	620 m^2/g

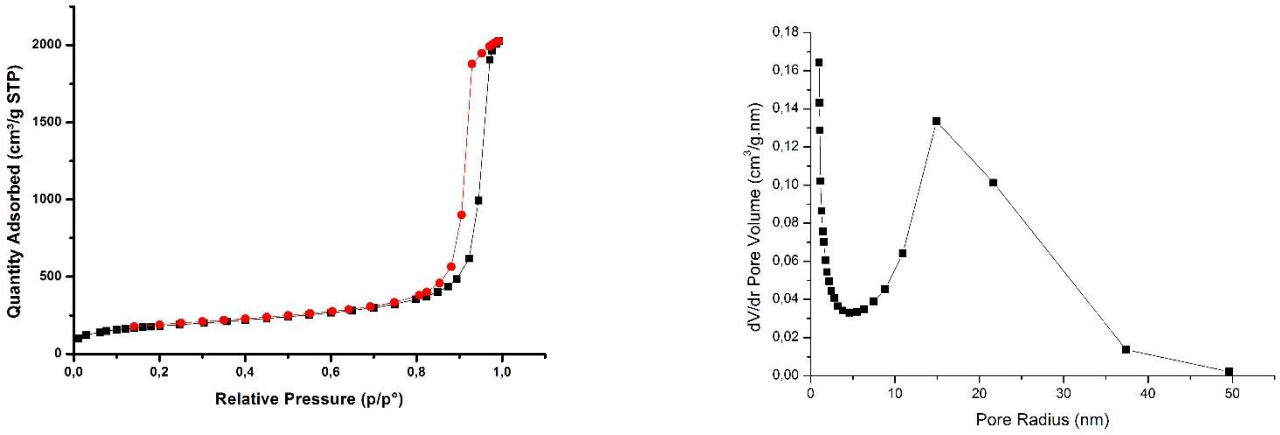

Figure 4-1: RFA BET Linear Isotherm Plot and Pore Size Distribution

Four composites which contain various volumetric ratios of RFA were prepared. Desired volumetric ratios of aerogels were adjusted before pressing the mixture of RFA and UF grains. Therefore the volumetric ratios were adjusted by first weighing RFA grains and then using the density of RFA before pressing to calculate the volume of RFA to be used. Percent volume of RFA used in the trials various from 10 to 38. Urea formaldehyde and RFA mixture was pressed at a pressure of 100 bars. Bulk density and the thermal conductivity of the resulting composites were measured and the results are reported in Figure 4-2.

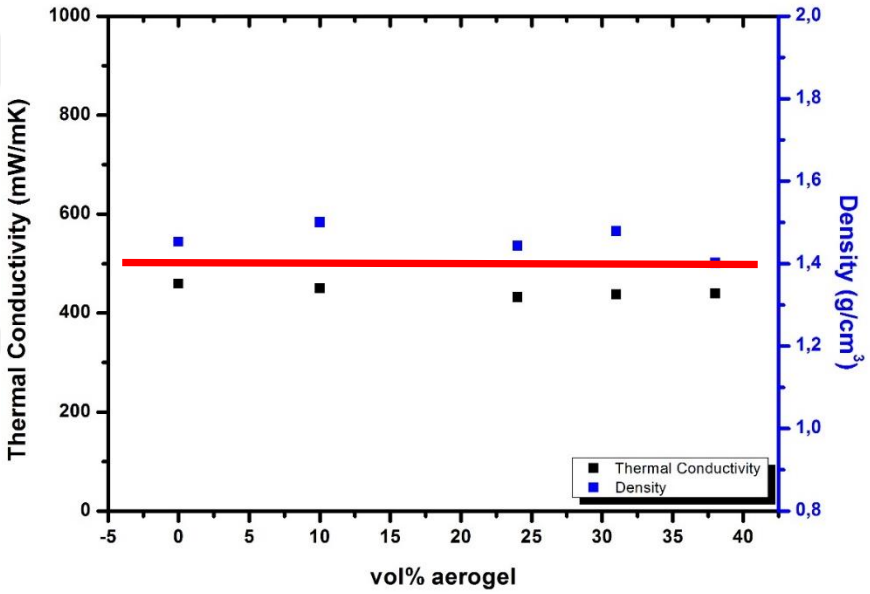

Figure 4-2: Thermal Conductivity and Density of the Composite prepared with RFA

Composites' density were close to the density of the native material, urea formaldehyde. No effect of changing aerogel percentage was observed on thermal conductivity. Even with the high aerogel percentage desired reduction in the density and thermal conductivity was not achieved. Density and thermal conductivity of composites almost fall in a straight line, a constant value as shown by the red line. The result of these composite trials indicated that the aerogel does not show the good thermal insulation behavior as it shows before pressing.

In order to investigate the structural changes of aerogels under pressure, a cold press which can work with a small sample volume (2-5 cc) was used. Using this method, the environment in the industrial size hot press was simulated. RFA was pressed under pressures ranging from 20 bars up to 100 bars. The time of exposure to the pressure was the same with the time of hot pressing the composite in the factory, 225 seconds. After pressing aerogels in cold press, samples were obtained in a pellet form as shown in Figure 4-3, (A). BET surface area and pore volume were measured for the pressed RFAs.

Table 6: Structural properties of RFA after being exposed to various pressures

Pressure	**Pore Diameter**	**S.A.**	**Porosity**
bar	**nm**	**m^2/g**	**%**
1	19	620	88
20	4.9	457	56
40	4.1	426	46
60	3.7	370	24
80	3.6	339	20
100	3.4	327	4

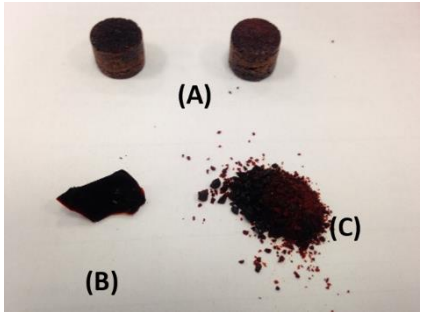

Figure 4-3:(A) Aerogel grains exposed to pressure, (B) Native aerogel, (C) crushed aerogel

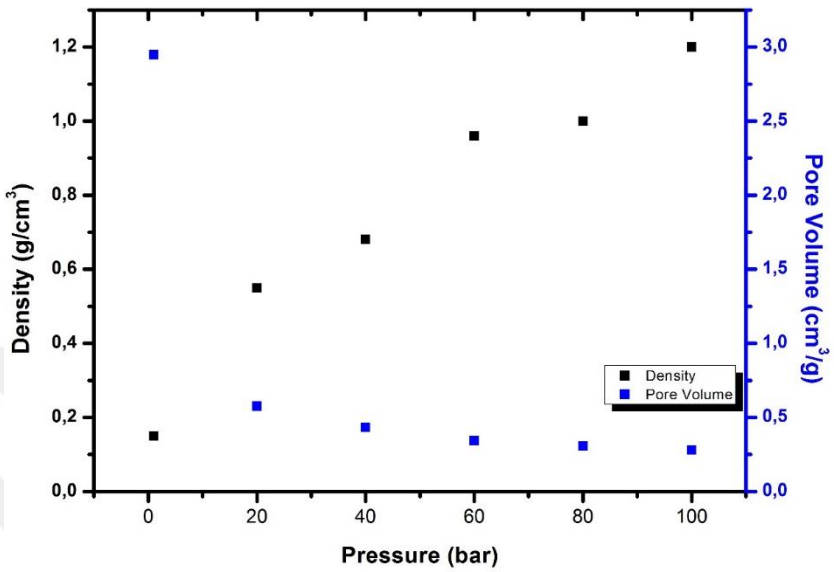

Figure 4-4: RFA density and pore volume change with pressure

The results of the cold press experiments indicate that aerogels lost their porosity significantly when they were exposed to pressure of 100 bars. The bulk density of RFA at 100 bars was close to the density of the backbone material, resorcinol formaldehyde resin. There was a significant reduction in the pore volume of the aerogel with increasing pressure. This reduction in the pore volume leads to a tremendous reduction in the gaseous thermal conductivity of the aerogel. However the high bulk density and low porosity brings the overall thermal conductivity of the aerogel close to the thermal conductivity of solid backbone material. The density change after the compression changes the volumetric ratios of UF and RFA in the composite. The effective thermal conductivity of a composite depends strictly on the volume fractions of materials which constitutes the composite [33]. Therefore the actual volume percentages of RFA in the composites were re-calculated by using the density of aerogels after being exposed to 100 bars. Results are given in Table 7.

Table 7: Calcualtion of actual RFA percentages in the composites

UF	RFA	RFA	vol%	vol% actual	UF Density	RFA (1Bar)	RFA (100Bar)
mL	*mL*	*g*	*Aerogel*	*Aerogel*	*g/mL*	*g/mL*	*g/mL*
1400	0	0	0	0	1.45	0.15	1.2
1300	150	22.5	10	2.05			
1100	350	52.5	24	5.45			
1000	450	67.5	31	7.54			
900	550	82.5	38	9.97			

The actual volume fractions of RFA in the composite varies between 0.02 and 0.1. The BET and bulk density measurements already indicated an expected increase in the overall thermal conductivity of RFA. The RFA with increased thermal conductivity constituted low volume of the composite. This explains why there was no significant change in the thermal conductivity and density of the composite compared to the native material, UF.

Aerogels with higher bulk densities can be synthesized to be used in the composites. High density aerogels could preserve their porosity better at high pressure since the high density of aerogels have better strength [7]. RFAs with higher densities can be synthesized by reducing the solvent amount and increasing the catalyst amount. Aerogels with higher densities have higher thermal conductivities. However if the pore structure can be preserved with these high density aerogels at high pressures, it is better to make UF composites with high density RFAs. Resorcinol formaldehyde aerogels with a density of 0.48 g/cm^3 (RFA-H) were synthesized.

Table 8: RFA-H Material Properties

Material Property	
Density	0.48 g/cm^3
Porosity	62%
BET S.A.	834 m^2/g

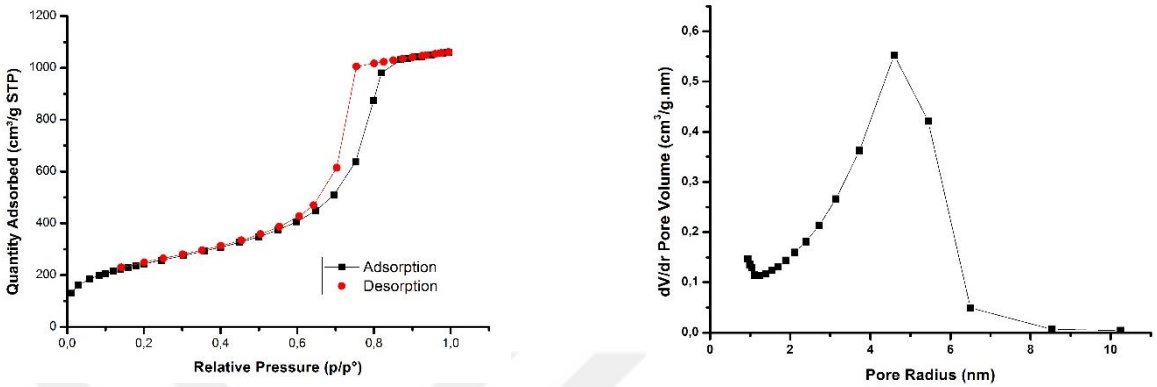

Figure 4-5: RFA-H BET Linear Isotherm Plot and Pore Size Distribution

Their behavior under pressure is investigated by again using a cold press. The results showed that denser aerogels were preserved their porosity better under pressure.

Table 9: Structural properties of RFA-H after exposure of various pressures

Pressure	Pore Diameter	S.A.	Porosity
bar	**nm**	**m^2/g**	**%**
1	7.63	834	62
20	3.0	433	21
60	2.4	240	20
100	2.1	189	17

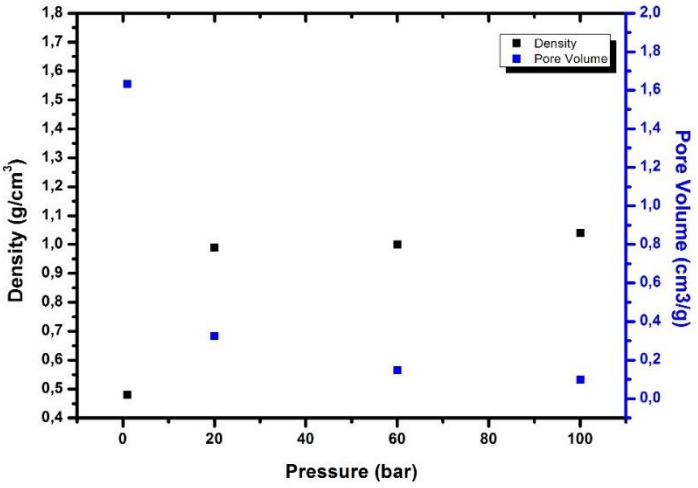

Figure 4-6: RFA-H density and pore volume change with pressure

Compared to lower density RFA, RFA-H preserved its porosity better at 100 bars. The bulk density of RFA-H is lower than the bulk density of the RFA at elevated pressures. At the production site, UF manufacture pressure were be able to reduce to 60 bars. Since the native material, UF, can be produced at 60 bars, this time the composite was also prepared at 60 bars. Only one composite with 30 vol% RFA-H was prepared. The volume percent of RFA-H in the composite was determined by weighing the RFA-H before the pressing and using the density after being exposed to 60 bars to find the volume. 30 cm x 30 cm composite were dived into 6 pieces with equal area. Thermal conductivity and density of these pieces were measured at different sides and places for several times. The standard deviation in the measurements of k and ρ was also reported. Also a plate pure UF was prepared and it had a thermal conductivity of 465 mW/mK and density of 1.45 g/mL. Percent decrease for k and ρ are based on these values.

Table 10: Thermal conductivity and density result for RFA-H and UF composite

	Thermal Conductivity	**Density**	**%decrease in k**	**%decrease in ρ**
	mW/mK	**g/cm^3**		
	349.91	1.28	24.7	10.4
Standard Deviation	25.83	0.07		

With the incorporation of 30 vol% of RFA-H nearly 25% decrease in the thermal conductivity was achieved. The standard deviation of density and thermal conductivity from the mean values reported in the table was around 5% both for the both properties. This small deviation implies that RFA-H was homogenously incorporated into the UF matrix. Heat capacity of the RFA-H based composite were theoretically calculated and it was 1092 J/K.kg. When the contact coefficients of UF and the composite were compared, 22% reduction in the heat flux at the surface was obtained. This can value can be correlated with the relative amount of warm sensation as discussed in the previous chapter.

The desired color of the toilet seat at the factory is shade of white. The manufacturer adopted this policy because their company research concludes that these colors give a sensation of cleanness. Color of resorcinol formaldehyde aerogels were dark violet as shown in the Figure 4-3. Water soluble dyes were added at the gel preparation step to synthesize RF gels with white color. Water soluble dye was chosen because the solvent used in the reaction medium of RFA synthesis was water. Dye was added into the reaction medium before gelation and it was mixed with the other reactants during polymerization process. Complete gelation was not achieved and a sand like texture was obtained as shown in Figure 4-7 (B). Attempts were made to incorporate zirconium, titanium and magnesium based pigments into the gel structure to manipulate the color of the gel. These pigment are commonly used in the coloring process of ceramics. However these attempts were unsuccessful since these pigments were not water soluble. In order to solve this problem during the gelation the mixture was continuously stirred to obtain gel structure with an evenly suspended pigments. At the end of gelation color of the RFA was dominant and again violet color gels were obtained.

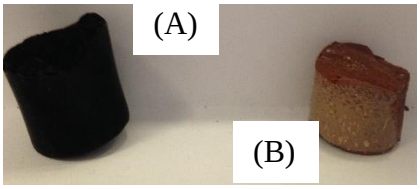

Figure 4-7: (A) Comparison of native RFA (B) RFA with the water soluble dye

Figure 4-8: Gels with precipitated zirconium pigment with varying weight percentages

4.2 UF-SA Composites

To overcome the color problem, silica aerogels were chosen. Silica aerogels are transparent or have a white cloudy color. Apart from their advantageous color for this project, they also possess low thermal conductivity. Solid thermal conductivity of SAs can be reduced tremendously with sol-gel process. Therefore even if the SA losses its porosity the compressed aerogel would have a low thermal conductivity.

Two different sets of silica aerogels were synthesized to be used in the UF based composite. First silica aerogel was prepared by increasing the precursor concentration without leaving the miscibility region of the reaction medium. The density of the silica aerogel (SA) obtained by this approach was 0.211 g/cm^3. The second set of silica aerogels (SA-H) were prepared by aging the gels in precursor based solution for two weeks and it had a density of 0.361g/cm^3. First composite trials were conducted by using SA. The pore size distribution were given in Figure 4-9. The porosity of SAs were around 90%. The structural changes for SA were investigated.

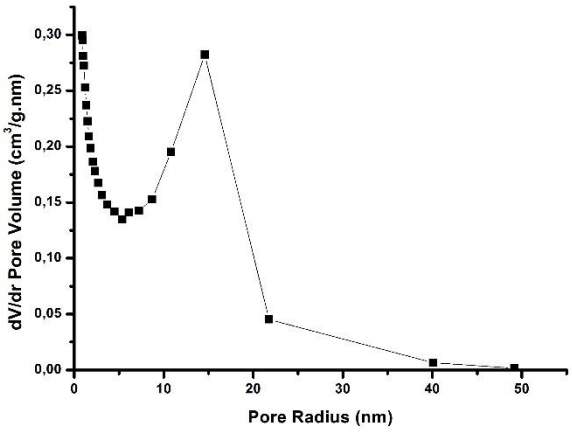

Figure 4-9: Pore size distribution of native SA

Table 11: Structural changes for SA at various pressures

Pressure	Pore Diameter	S.A.	Porosity	Pore Volume	Density
bar	nm	m^2/g	%	g/cm^3	g/cm^3
1	18	1057	90	4.75	0.211
20	3.82	917	67	0.90	0.736
60	1.33	689	12	0.06	1.945

There is a significant reduction in porosity when a pressure of 60 bars was applied. However the bulk density of the pressurized sample differed by 11% from the solid backbone density. This means that the suppression in solid thermal conductivity was still present. There was a considerable loss in the pore volume. The gaseous thermal conductivity effect would become negligible for this pore size and pore volume [7, 23]. Two composites with 23 and 8 vol% of SA were prepared. Thermal conductivity of pure UF plate in this trial were measured as 470 mW/mK and the density was 1.45 g/cm^3.

Table 12: UF and SA with two different volumetric fractions

	Thermal Conductivity	SD in $k_{composite}$	Density	SD in ρ	%decrease in k	%decrease in ρ
	mW/mK		g/cm^3			
23 vol% Silica Aerogel	366.45	12.55	1.33	0.07	28	7.98
8 vol% Silica Aerogel	450.83	11.17	1.43	0.02	4	1.52

With just 23 vol% of SA nearly 30% reduction in the thermal conductivity was achieved. Standard deviations for thermal conductivity and density once again proved the even distribution of SA in UF matrix. The heat capacity of 8 vol% and 23 vol% composites were 1160 J/K.kg and 1085 J/K.kg respectively. 20% reduction in the heat flux at the surface for the 23 vol% SA composite was achieved. Compared to the composite of RFA-H (30 vol %), greater reduction in the heat flux was achieved, even though the SA had lower porosity at 60 Bar compared to the

RFA-H. This increased reduction in heat flux was due to the lower backbone thermal conductivity of SA at 60 Bar. The composite with low volume fraction of SA, 8 vol%, exhibited only 4% reduction in the heat flux.

In order to preserve porosity better, trials with SA-H were conducted. The structural changes of SA-H under pressure is reported in Table 13. Nearly 1 kg of SA-H was synthesized to be used in composite trials as shown in the Figure 4-10.

Figure 4-10: 950 grams of SA-H

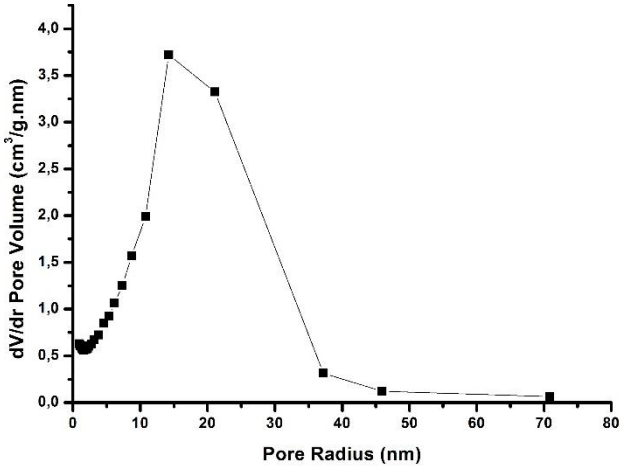

Figure 4-11: Pore size distribution of native SA-H

Table 13: Structural changes for SA-H at various pressures

Pressure	Pore Diameter	S.A.	Porosity	Pore Volume	Density
bar	nm	m^2/g	%	g/cm^3	g/cm^3
1	13.37	741	84	2.55	0.361
20	5.94	728	71	1.11	0.640
60	3.57	642	56	0.59	0.962

Porosity of SA-H was preserved better compared to SA. TEOS aging of silica aerogel reinforced the mechanical properties of SA-H. The density increase with pressure was lower compared to the SA's results. Four composites with different SA-H volume percentages were prepared. Their thermal conductivity and density are given in the figure below.

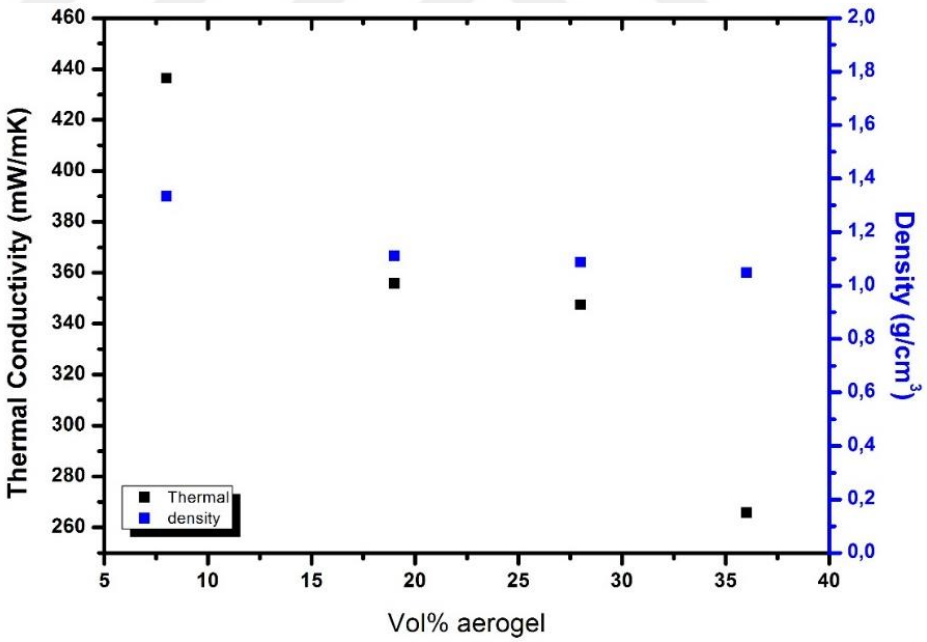

Figure 4-12: Thermal conductivity and density change with increasing SA-H aerogel volume

Table 14: UF and SA-H with two different volumetric fractions

Silica aerogel in the composite	Thermal Conductivity	SD in $k_{composite}$	Density	SD in ρ	%decrease in k	%decrease in ρ
vol%	**mW/mK**		**g/cm^3**			
8	436.36	14.18	1.33	0.04	9	8
19	355.86	15.92	1.11	0.07	26	23
28	347.50	28.88	1.09	0.08	28	25
36	265.78	13.98	1.05	0.04	43	28

Even with a 8 vol% of aerogel nearly 10% reduction in thermal conductivity was obtained. With higher SA-H volume in the composite percent reduction in thermal conductivity was increased. A sudden drop in the thermal conductivity of composite were observed for the composite with 36 vol% SA-H. Since the filler amount was increased in the matrix, more SA-H particles became in contact with each other. They produced gate-ways in the UF matrix which were highly resistant to heat flow especially compared with urea-formaldehyde [33]. The struggle of heat to go through the regions with high SA-H concentration can be the reason for the sudden drop in the thermal conductivity.

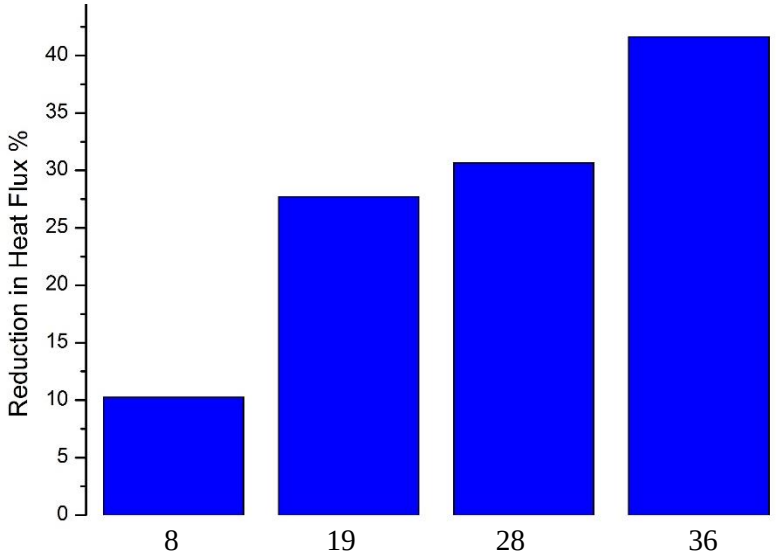

Figure 4-13: % reduction of heat flux for SA-H composites of UF

Heat capacity of the composites were 1020, 1060, 1105 and 1160 J/K.kg. The composites reduced the heat flux at the surface up to 42% compared to the native material. This value was achieved by using 36 vol% of SA-H. Summary of the %reduction of heat flux was presented in Figure 4-15.

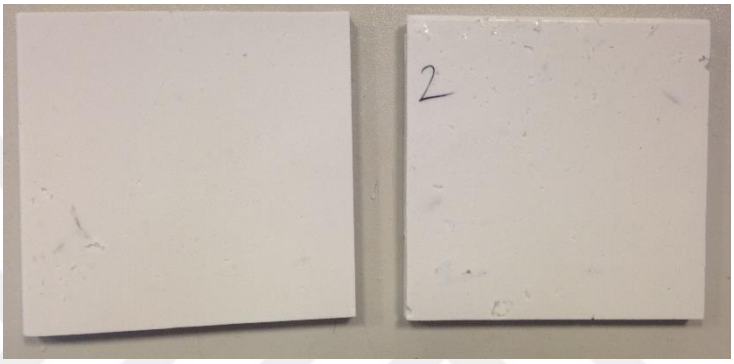

Figure 4-14: SA-H and UF composite with 8 vol% and 28 vol% SA-H

4.3 Effective Thermal Conductivity Models

There was a decrease in the thermal conductivity of aerogels after they were exposed to the pressure of the hot press. Therefore to determine the thermal conductivity of silica and resorcinol formaldehyde aerogels correlation between the aerogel density and the thermal conductivity were used. As discussed earlier the radiative thermal conductivity of organic aerogels does not contribute appreciably to the overall thermal conductivity of aerogels. The pore size and the pore volume of the pressed aerogels exhibited radical decrease in their values as compared to aerogels before pressed. Therefore gaseous and radiative thermal conductivity of pressed aerogels were ignored. The bulk density of resorcinol formaldehyde aerogels, RFA and RFA-H, at 60 bar was close the solid backbone density (1.25 g/cm^3) of the aerogels. The solid thermal conductivity of RFA increases exponentially with the increasing bulk density. Therefore the solid thermal conductivity of the resorcinol formaldehyde aerogels which were exposed to the pressure of 60 bar was assumed to have the same thermal conductivity with the solid

backbone. For silica aerogels even for relatively high densities solid thermal conductivity is suppressed compared to the backbone materials thermal conductivity [7, 23]. Ebert has collected solid thermal conductivity data for silica aerogels at different densities and constructed a graph to show the relation between the ratio of backbone thermal conductivity and the solid fraction of the aerogel [7]. The solid thermal conductivity of silica aerogels which were pressed under 60 bar was determined from this relation. Density and thermal conductivity of aerogels after being pressed are summarized in Table 15.

Table 15: Thermal Conductivities of Aerogels after being pressed

Aerogel	**Density after Pressing**	**Solid Thermal Conductivity**
	g/cm^3	**mW/mK**
RFA-17*	1.20	128.0
RFA-H	1.10	128.0
SiO_2-L	1.95	126.4
SiO_2-H	0.94	113.8

*pressed at 100 bars

The volumetric fraction of the UF and aerogel in the composited was calculated by using the densities of these materials after they were exposed to the manufacture pressure. The volumetric fractions of RFA was low and close to each other in the first composite. Therefore the thermal conductivity measurement results were close to each other. Effective thermal conductivity of RFA-H, SA and SA-H composites were calculated. Experimentally determined thermal conductivities were compared with the predictions of the models. Results are presented in Table 16. %off shows the deviation of the models output from the experimental result.

Table 16: Effective Thermal Conduction Prediction with various models

			Rayleigh		Maxwell		EMT		Levy	
vol%	**Aerogel**	**k_{exp}**	**k**	**%off**	**k**	**%off**	**k**	**%off**	**k**	**%off**
30	**RFA-5**	349.91	343.73	-1.77	343.32	-1.88	383.57	9.62	329	-5.98
8	**SiO_2-L**	450.83	434.58	-3.61	434.57	-3.61	434.01	-3.73	428.84	-4.88
23	**SiO_2-L**	366.45	372.87	1.75	372.73	1.71	368.82	0.64	360.18	-1.71
8	**SiO_2-H**	436.36	432.25	-0.94	432.25	-0.94	432.23	-0.95	425.36	-2.52
19	**SiO_2-H**	355.86	384.35	8.01	384.39	8.02	381.65	7.25	370.98	4.25
28	**SiO_2-H**	347.5	347.45	-0.02	347.64	0.04	341.75	-1.65	331.05	-4.73
36	**SiO_2-H**	265.77	316.10	18.94	316.65	19.14	307.67	15.77	298.60	12.35

Effective thermal conductivity predictions of Rayleigh and Maxwell models were in quite in agreement in terms of their prediction for all composites. This is because Rayleigh's model modifies the Maxwell Model to include the effect of interaction of dispersed spheres in the continuous matrix. Rayleigh considers the simple cubic arrangement of filler in the continuous matrix, whereas Maxwell model assumes dilute insertion of spherical particles. Therefore the results of the two model approaches to each other at low volumetric fractions [47]. Their slight disagreement as the vol% of aerogel increases were observed for the composite with SA-H.

RFA-H and UF composite's thermal conductivity was best predicted with the Rayleigh and Maxwell Models. EMT model assumes complete random dispersion of the filler particles in the composite. Maxwell-Eucken (M-E) is a modified version of the Maxwell model to include more filler particles. M-E has two forms where a material can be a continuous phase in one or a filler in another one. Levy's model is an algebraic manipulation of these two models which gives good predictions for well dispersed phase with high volumetric fractions. The predictions of EMT and Levy's model were a bit more off from the experimental result since the composite only contained a volume fraction of 0.3 aerogel. For SA composite as the aerogel volume fraction increased, predictions of EMT and Levy's model got closer to the experimental result. For the 8 vol% SA Maxwell and Rayleigh models gave reasonable good results.

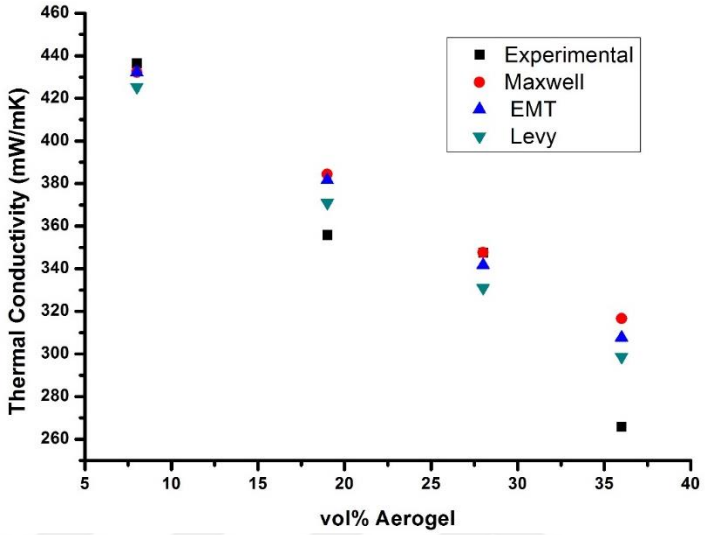

Figure 4-15: Effective thermal conductivity prediction of SiO2-H composites

8 vol% and 28 vol% SA-H based composites' effective thermal conductivity had good agreement with the Maxwell Model. 19 vol% composite shows deviation from all the models that were used. However the thermal conductivity of the pieces obtained from this composite had a larger standard deviation compared. This high standard deviation can be due to the fact that aerogels were not evenly distributed in the sample. Some might be dispersed quite well on the surface of the composite as well as it was incorporated within the sample. The higher deviation from the models was also observed for the composite with 36 vol% aerogel. The percolation threshold is usually observed for the composites with fillers which have quite different thermal conductivity at high volume fractions of filler [33]. The composite with porous silica aerogels with 0.36 volume fraction might have reached the threshold. Therefore the model's predictions did not agree with the experimental data.

Chapter 5 Conclusion

Aerogel based composites of urea formaldehyde were produced to obtain toilet seats with warm feeling. Amount of heat flux at the surface of the composite were correlated with the sensation of warmth. Contact coefficient which was function of thermal conductivity, density and heat capacity was used to determine the extent of warm sensation. Composites were prepared by using resorcinol formaldehyde and silica aerogels in industrial size hot press. The structural changes in aerogels which occurred at the manufacture pressure were determined using BET analysis and bulk density measurements. The analysis made on the pressed aerogels showed that denser aerogels were needed to preserve the structural and thermal properties of aerogels under pressures. Dense silica aerogel (0.361 g/cm^3) and dense resorcinol formaldehyde aerogel (0.48 g/cm^3) were successfully reduced the thermal conductivity and the density UF at 60 bars. Heat flux on the surface of composites reduced up to 40% compared to the native urea formaldehyde plates. Thermal conductivity of pressed aerogels were predicted by using correlations which relate density with the aerogel thermal conductivity. Effective thermal conductivity of composites were also predicted with models and results were compared with the experimental data. Maxwell and Rayleigh's model gave thermal conductivity predictions that reasonable agree with the experimental results for composites with low density silica aerogels and high density resorcinol formaldehyde aerogels. The thermal conductivity of high density silica aerogel were best predicted by EMT.

REFERENCES

1. Ho, H.N. and J.A. Jones, *Development and Evaluation of a Thermal Display for Material Identification and Discrimination.* ACM Transactions on Applied Perception, 2007. **4**(2).
2. Jones, L.A. and H.N. Ho, *Warm or Cool, Large or Small? The Challenge of Thermal Displays.* Ieee Transactions on Haptics, 2008. **1**(1): p. 53-70.
3. Kajimoto, H., S. Saga, and M. Konyo, *Pervasive Haptics Science, Design and Application*. 2016: Springer.
4. Tiest, W.M.B., *Tactual perception of liquid material properties.* Vision Research, 2015. **109**: p. 178-184.
5. Verrillo, R.T., et al., *Effects of hydration on tactile sensation.* Somatosensory and Motor Research, 1998. **15**(2): p. 93-108.
6. Harper, C.A., *Modern Plastics Handbook*. 2000: McGraw Hill Professional.
7. Aegerter, M.A., et al., *Aerogels Handbook*, in *Advances in sol-gel derived materials and technologies*. 2011, Springer Science+Business Media, LLC,: New York. p. 1 online resource (xxxi, 932 p.
8. Al-Muhtaseb, S.A. and J.A. Ritter, *Preparation and properties of resorcinol-formaldehyde organic and carbon gels.* Advanced Materials, 2003. **15**(2): p. 101-+.
9. Dorcheh, A.S. and M.H. Abbasi, *Silica aerogel; synthesis, properties and characterization.* Journal of Materials Processing Technology, 2008. **199**(1-3): p. 10-26.
10. Darian-Smith, I. and K.O. Johnson, *Thermal sensibility and thermal receptors.* Journal of Investigative Dermatology, 1977. **69**: p. 146-153.
11. Berris, M.J., *Development of a thermal device for a haptic display*. 2002, Massachusetts Institute of Technology. p. 74 leaves.
12. Ino, S., et al., *A Basic Study on the Tactile Display for Telepresence.* Ieee International Workshop on Robot and Human Communication : Proceedings, 1992: p. 58-62.
13. Kawabata, S., *The Standardisation and Analysis of Hand Evaluation.* Textile Machinery Society of Japan, 1980.
14. Yoneda, M.a.K., S., *Analysis of Transient Heat Conduction and Its Applications, Part II.* J. of Textile Mach. Soc. Jpn., 1985.
15. Rowe, J.L. and Building and Fire Research Laboratory (U.S.), *The impact of thermal imaging camera display quality on fire fighter task performance*, in *Nist Gcr 09-926*. 2009, U.S. Dept. of Commerce, National Institute of Standards and Technology,: Gaithersburg, Md.

16. Sarde, A., Deterre, R. , Vergneault, C., *Heat perception measurements of the different parts found in a car passenger compartment.* Measurement 2003. **35**: p. 65-75.
17. SS, K., *Coherent Expanded Aerogels and Jellies.* Nature, 1931. **127**: p. 741.
18. Pekala, R.W., *Organic Aerogels from the Polycondensation of Resorcinol with Formaldehyde.* Journal of Materials Science, 1989. **24**(9): p. 3221-3227.
19. Lin, C. and J.A. Ritter, *Effect of synthesis pH on the structure of carbon xerogels.* Carbon, 1997. **35**(9): p. 1271-1278.
20. Fricke, J. and T. Tillotson, *Aerogels: Production, characterization, and applications.* Thin Solid Films, 1997. **297**(1-2): p. 212-223.
21. Sanli, D. and C. Erkey, *Effect of polymer molecular weight and deposition temperature on the properties of silica aerogel/hydroxy-terminated poly(dimethylsiloxane) nanocomposites prepared by reactive supercritical deposition.* Journal of Supercritical Fluids, 2015. **105**: p. 99-107.
22. Hrubesh, L.W. and R.W. Pekala, *Thermal-Properties of Organic and Inorganic Aerogels.* Journal of Materials Research, 1994. **9**(3): p. 731-738.
23. Fricke, J., et al., *Thermal-Properties of Silica Aerogels.* Journal De Physique, 1989. **50**(C-4): p. C487-C497.
24. Lu, X., et al., *Thermal-Conductivity of Monolithic Organic Aerogels.* Science, 1992. **255**(5047): p. 971-972.
25. Hrubesh, L.W., *Aerogel applications.* Journal of Non-Crystalline Solids, 1998. **225**(1-3): p. 335-342.
26. Fricke, J., et al., *Optimization of Monolithic Silica Aerogel Insulants.* International Journal of Heat and Mass Transfer, 1992. **35**(9): p. 2305-2309.
27. Yoldas, B.E., M.J. Annen, and J. Bostaph, *Chemical engineering of aerogel morphology formed under nonsupercritical conditions for thermal insulation.* Chemistry of Materials, 2000. **12**(8): p. 2475-2484.
28. Zeng, S.Q., A. Hunt, and R. Greif, *Theoretical Modeling of Carbon Content to Minimize Heat-Transfer in Silica Aerogel.* Journal of Non-Crystalline Solids, 1995. **186**: p. 271-277.
29. Ebewele, R.O., *Polymer Science and Technology*. 1996, New York: CRS Press LLC.
30. Sanli, D. and C. Erkey, *Monolithic Composites of Silica Aerogels by Reactive Supercritical Deposition of Hydroxy-Terminated Poly(Dimethylsiloxane).* Acs Applied Materials & Interfaces, 2013. **5**(22): p. 11708-11717.
31. Ulker, Z. and C. Erkey, *An emerging platform for drug delivery: Aerogel based systems.* Journal of Controlled Release, 2014. **177**: p. 51-63.
32. Ristic-Lehmann, C., et al., *Aerogel/PTFE composite insulating material*. 2005: USA.

33. Pietrak, K. and T.S. Wisniewski, *A review of models for effective thermal conductivity of composite materials.* Journal of Power Technologies, 2015. **95**(1): p. 14-24.
34. Xu, J.Z., B.Z. Gao, and F.Y. Kang, *A reconstruction of Maxwell model for effective thermal conductivity of composite materials.* Applied Thermal Engineering, 2016. **102**: p. 972-979.
35. Wang, J., et al., *A new structural model of effective thermal conductivity for heterogeneous materials with co-continuous phases.* International Journal of Heat and Mass Transfer, 2008. **51**(9-10): p. 2389-2397.
36. Wang, J.F., et al., *A new approach to modelling the effective thermal conductivity of heterogeneous materials.* International Journal of Heat and Mass Transfer, 2006. **49**(17-18): p. 3075-3083.
37. Pham, Q.T. and J. Willix, *Thermal-Conductivity of Fresh Lamb Meat, Offals and Fat in the Range -40-Degrees-C to +30-Degrees-C - Measurements and Correlations.* Journal of Food Science, 1989. **54**(3): p. 508-515.
38. Gong, L.L., et al., *A novel effective medium theory for modelling the thermal conductivity of porous materials.* International Journal of Heat and Mass Transfer, 2014. **68**: p. 295-298.
39. Brunauer, S., P.H. Emmett, and E. Teller, *Adsorption of Gases in Multimolecular Layer.* Journal of the American Chemical Society, 1938. **2**: p. 309–319.
40. Yi, H., *Rapid thermal conductivity measurement with a hot disk sensor - Part 1. Theoretical considerations.* Thermochimica Acta, 2005. **436**(1-2): p. 122-129.
41. Yi, H., *Rapid thermal conductivity measurement with a hot disk sensor - Part 2. Characterization of thermal greases.* Thermochimica Acta, 2005. **436**(1-2): p. 130-134.
42. Atkins, P.W. and J. De Paula, *Atkins' Physical chemistry*. 8th ed. 2006, Oxford ; New York: Oxford University Press. xxx, 1064 p.
43. Riviere, L., et al., *Specific heat capacity and thermal conductivity of PEEK/Ag nanoparticles composites determined by Modulated-Temperature Differential Scanning Calorimetry.* Polymer Degradation and Stability, 2016. **127**: p. 98-104.
44. Sachithanadam, M. and S.C. Joshi, *Silica aerogel composites : novel fabrication methods*, in *Engineering Materials,*. 2016, Springer,: Singapore. p. 1 online resource (xii, 139 pages).
45. Miyoshi, T., et al., *Aluminum foam, "ALPORAS": The production process, properties and applications.* Porous and Cellular Materials for Structure Applications, 1998. **521**: p. 133-137.
46. Brittain, H.G., *The Oxide Handbook, 2nd Edition - Samsonov,Gv.* Journal of the American Chemical Society, 1983. **105**(8): p. 2514-2514.

47. Bird, R.B., W.E. Stewart, and E.N. Lightfoot, *Transport phenomena*. 2nd ed. 2002, New York: J. Wiley. xii, 895 p.